Optimization of Superconducting Cavities: Shape, Fields, Multipactor

Valery D Shemelin,

CLASSE, Cornell University

What does the world want today?

- ILC wants high gradient (31.5 MV/m is the base line of the project, but 40, 50 MV/m – who will mind?)
- ERL wants moderate gradients (20 MV/m) but low losses (refrigerator)
- Industrial linacs can have even less gradients but high Q for conductive cooling
- What are the issues for each application?
- How do we design the cavity cells to make these issues less problems?

Outline

- Superconducting accelerating cavity
  What defines the shape of cells?
- Cell geometry: (2-)elliptic cells, peak fields and losses
  Figures of merit *E*pk/*E*acc, *Hpk/Eacc*, *GR/Q*
- Optimization: Success with Reentrant cells (min Hpk/Eacc for a given Epk/Eacc)
- Analysis: Defining parameters: aperture, wall slope angle, *E*pk/*E*acc
- Inner and end cells. Transitions to the beam pipe
- Non-elliptic cavity shapes
- Equidistant optimization
- SLANS et al. Comparison of codes. Envelope codes: TunedCell, TunedCellEnd, TunedCellSingle
- Procedure of optimization
- Multipactor in elliptic cavities. MP-free transitions to beam pipes
- Conclusions

Superconducting accelerating cavity: what defines the shape of cells?

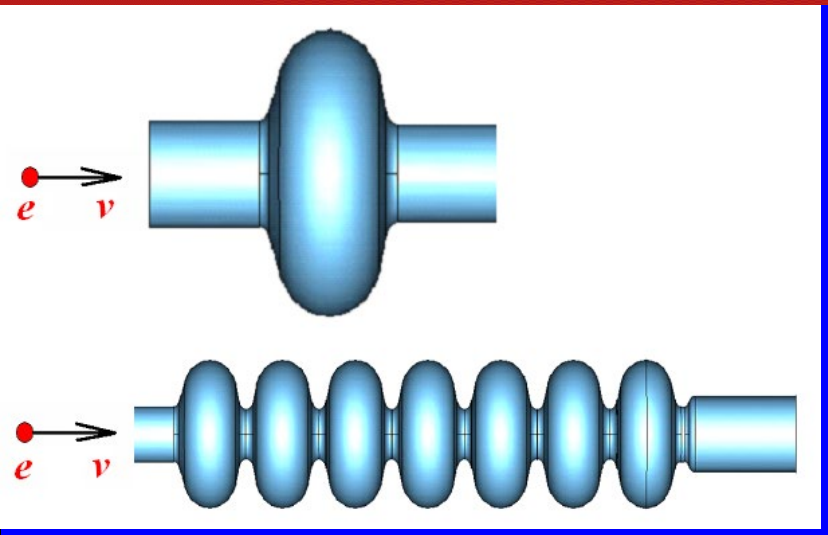

Single cell and multicell elliptical cavities. Transitions to the beam-pipe can be of different shape to improve propagation of the HOMs: some HOMs can be extracted to the leftt, some of them - to the right.

- Evolution: earlier superconducting cavities suffered from multipacting. The invention of round-wall cavities (P. Kneisel et al.) allowed a significant performance improvement.
- One can afford to make a beam hole for a SC cavity much larger than for a NC cavity where power dissipation is a major concern, instead we have reduced *R/Q* for Higher Order Modes and can have higher currents.
- Transitions between cells and to the beam pipe should be smooth to decrease the *E*pk.
- Equatorial region should be rounded to increase *Q* and, as it turned out, to mitigate multipacting.

Good approach for the shape of a SC half-cell is a two-elliptic-arc curve with a straight segment between arcs.

Cell geometry: Figures of Merit

- I will discuss the Figures of Merit : *E*pk/*E*acc, *H*pk/*E*acc and *GR/Q*, and their dependence on the dimensions of the cell.

  They depend on the shape only (not on the size, i.e. not on the frequency).

- *E*pk/*E*acc and *H*pk/*E*acc define maximal fields on the surface of the cavity. They are responsible for X-radiation (field emission) and thermal breakdown (quench).

- The value of *GR/Q* defines losses for a given *R*s (residual surface resistance) and should be chosen as big as possible.

- Values of *R*a (iris aperture) define cell-to-cell coupling and we will state only that coupling increases for reentrant cells (that is good).

Other values (HOM's impedances, or wake-fields) are connected with the whole multicell cavity structure and are beyond the scope of this report. However, *R/Q* for HOMs depends strongly on the shape of the end cells.

$$G = \frac{\omega_0 \mu_0 \int_V |\mathbf{H}|^2 \, dv}{\int_S |\mathbf{H}|^2 \, ds}.$$

$$P_c = \frac{V_{cav}^2}{R_{sh}} = \frac{V_{cav}^2}{Q_0 \cdot (R_{sh}/Q_0)} = \frac{V_{cav}^2}{(R_s \cdot Q_0) \cdot (R_{sh}/Q_0)/R_s} = \frac{V_{cav}^2 \cdot R_s}{G \cdot R_{sh}/Q_0}.$$

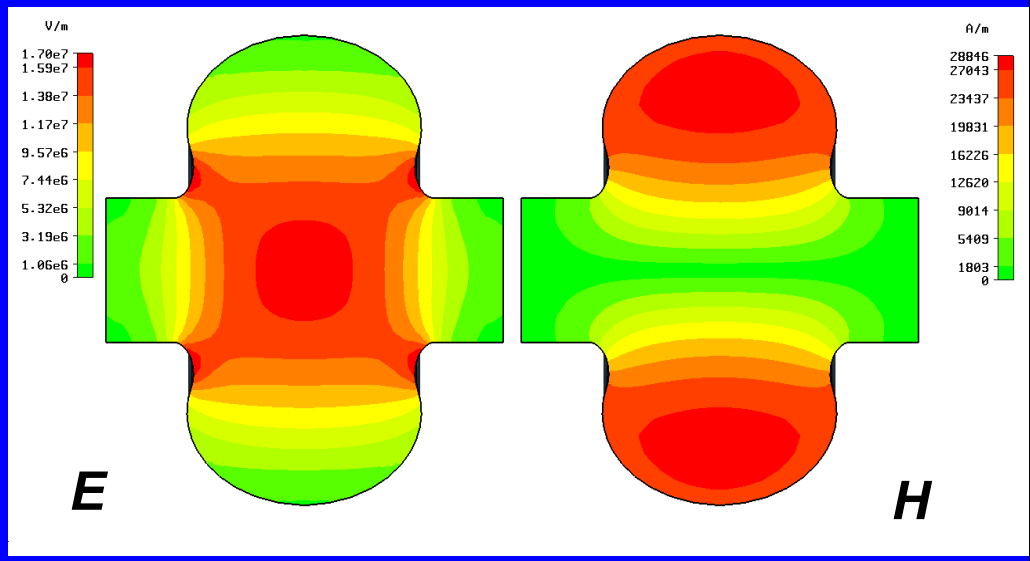

Fields in a reentrant cavity. Ra = 30 mm

Goals of Cavity Shaping

Critical magnetic field is a hard limit for *H*pk at which superconductivity fails and the cavity quenches;

whereas *E*pk is a soft limit: field emission can be decreased by better cleanliness and high power processing

Goals :

- Reduce *H*pk/*E*acc for high gradient applications like ILC
- Increase *GR/Q* for CW moderate field applications like ERL, to reduce the size of the refrigerator $$$.
- Sacrifice *E*pk/*E*acc if necessary
- Make sure you do not create MP troubles (you should always watch it out!)

Cell geometry: (2)-elliptic cells

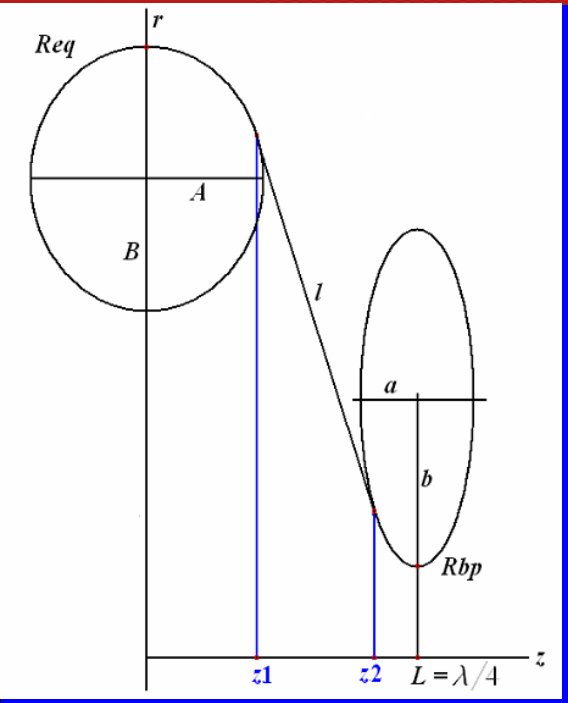

- Transition to the 2-elliptic-arc shape with tilted end plates for Nb cavities was proposed by J. Halbritter, 1980.
- P. Kneisel et al (1981) presented first results with such a cavity and showed that residual losses (*Rs/G*) decrease, and many other properties improve: easier fabrication, mechanical stability, reduction of chemical residues, *E*pk/*E*acc compared to spherical cavity with the same cell-to-cell coupling, no multipacting in first calculations, FE electrons drift out through the beam hole, coupling of TM01*n* modes increases with *n* easing damping of HOMs.
- Systematical analysis of reducing the peak electric field by shaping the iris edge in an ellipse has been done to this time (M. Karliner et al., 1986)
- Analysis of shaping the equatorial region for lower magnetic field led us to an elliptic reentrant cavity (V. Shemelin, H. Padamsee, 2002)

•The 2-elliptic cell has 7 dimensions that define its shape but only 4 of them are independent. *L* is defined by frequency, *Rbp* (or *Ri* – iris aperture) is given from other considerations, and *Req* is used for tuning to the chosen frequency. The length of the straight segment *l* is defined as the length of a tangential segment between two ellipses. Axes of the ellipses are parallel to axes of coordinates *z* and *r*.

Alternative system of geometrical parameters

- Some authors, starting from [*] use a different system of geometrical variables for optimization:

- B/A , the equator ellipse aspect ratio;	defines a local min of the peak surf. mag. field;
- b/a, the iris ellipse aspect ratio;	defines a local min of the peak surf. el. field;
- d, the wall distance from the iris plane;	allows the trade-off between m. and e. fields;
- γ, the wall angle inclination;	influence the mechanical stiffness, controls the inductive volume of the cavity.

- I believe that my system is more convenient because all the primary variables (A, B, a, b –half-axes of the ellipses) are uniform. Dependences on Ri, α, and Epk/Eacc are monotone (as will be shown later) and can be easily understood from the presented graphs.

- Method of optimization with these 4 variables (A, B, a, b) leads to a final exact result under chosen limitations (Ri, α, Epk/Eacc, β = v/c), while another optimization has an estimative quality.

- *P. Pierini et al., Cavity design tools… , Proc. 9th workshop on SRF, 1999.
- Sang-Ho Kim et al. Efficient Design Scheme of Superconducting Cavity. Linac 2000.

Two-elliptic cells: *E*pk vs *H*pk

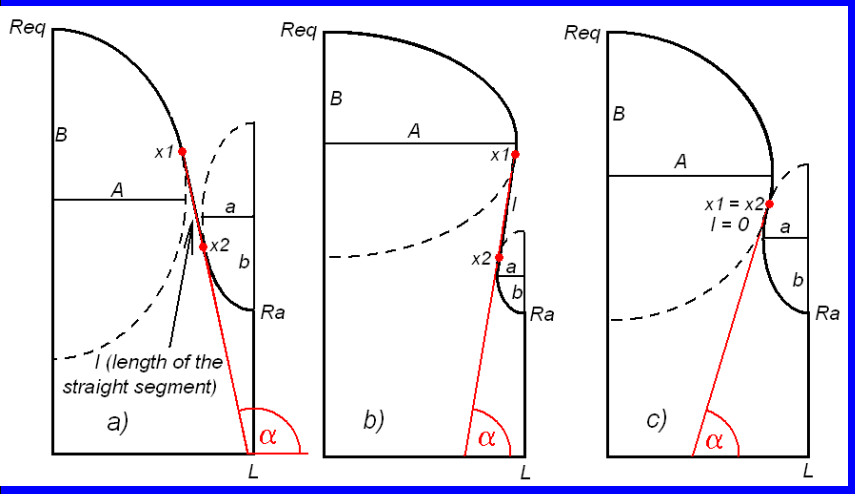

- Given the aperture (*R*a), one more physical parameters can be taken as predetermined: the value of *E*pk/*E*acc.*
- In this case we can vary the whole array of half-axes (*A, B, a, b*) choosing between them those which correspond to the given *E*pk/*E*acc and find the lowest value of *H*pk/*E*acc or the highest of *GR/Q* depending on the goal to be sought.

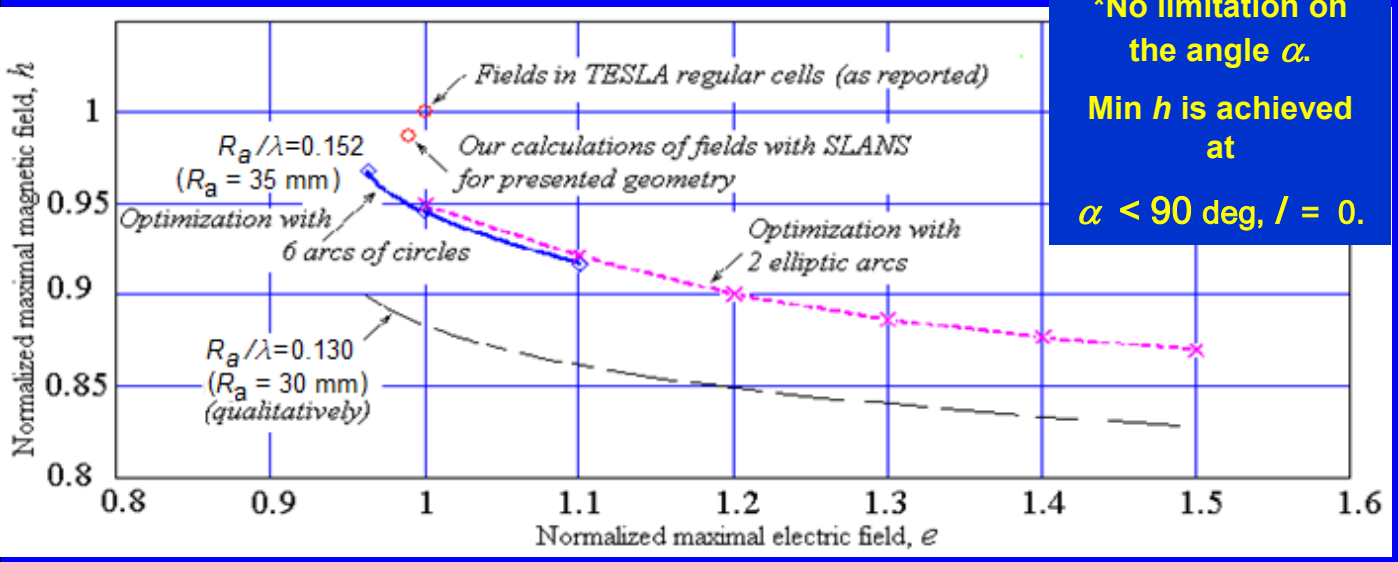

*No limitation on the angle α.

Min *h* is achieved at

α < 90 deg, *l* = 0.

•In the case of *H*pk/*E*acc we obtain the curve shown here (*GR/Q* – later). For normalization, values of TESLA inner cell are taken: *e* = *E*pk/2*E*acc, *h* = *H*pk/42*E*acc, so that for TESLA *e* = 1 and *h* = 1.

Two-elliptic cells, appearance of reentrant cells

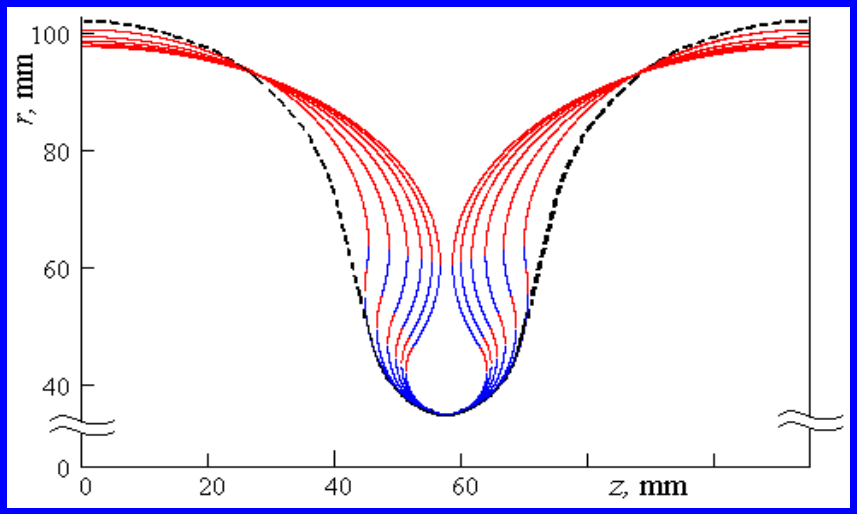

Optimization of the TESLA regular cell shape.

Dashed line – the present shape, solids - optimization with 2 elliptic arcs, δe = 0, 10, …, 50 %.

In search of lowest magnetic field for given electric field we came to the shapes shown here: reentrant shapes

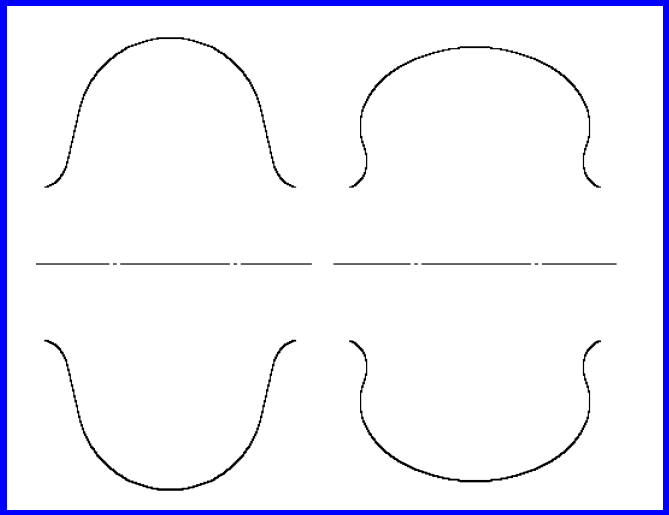

From the previous slide we chose the point with 10 % lower magnetic field sacrificing 20 % electric field

Left – original TESLA inner cell

Right – the chosen cell

The length of the straight segment turned out to be zero.

Comparison of some cells…

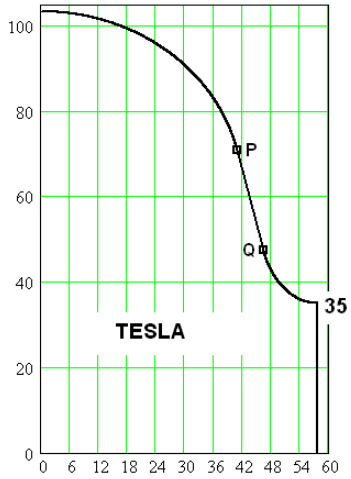

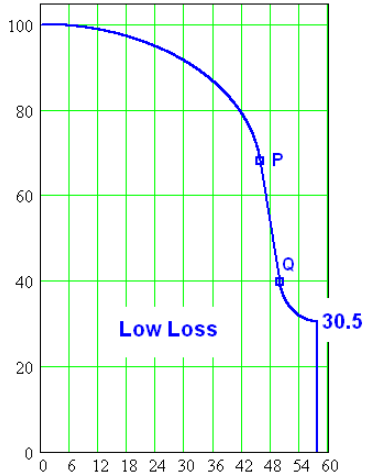

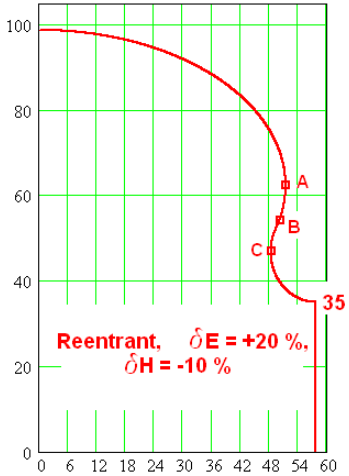

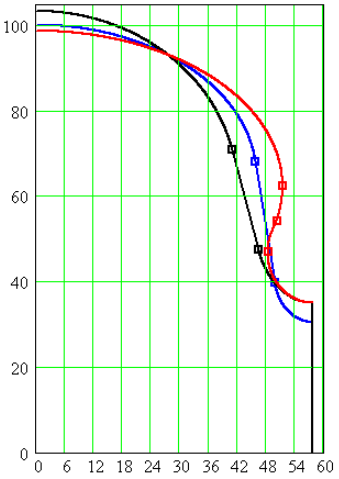

…their electric field along the profile line

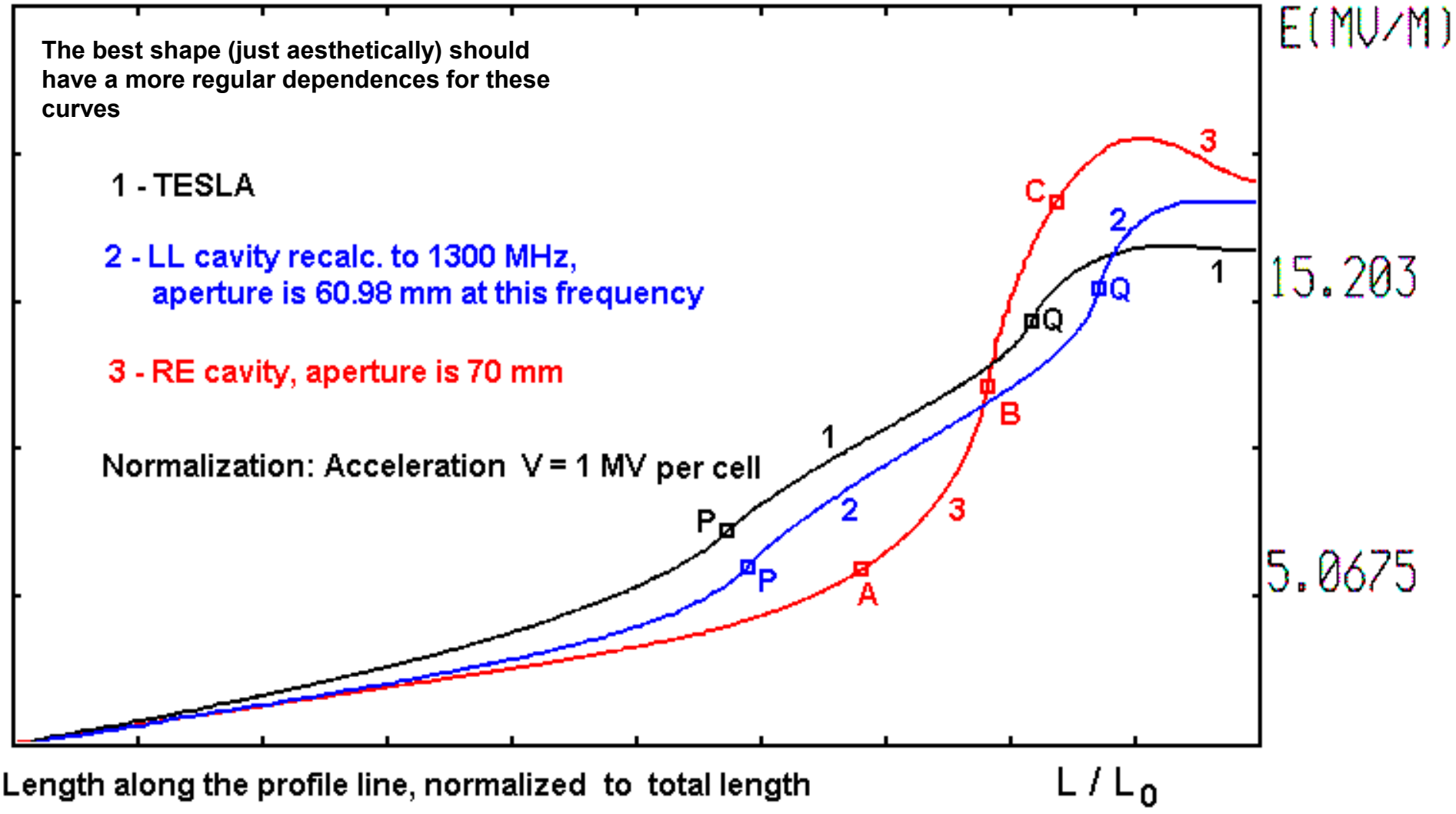

…and magnetic field on the profile line

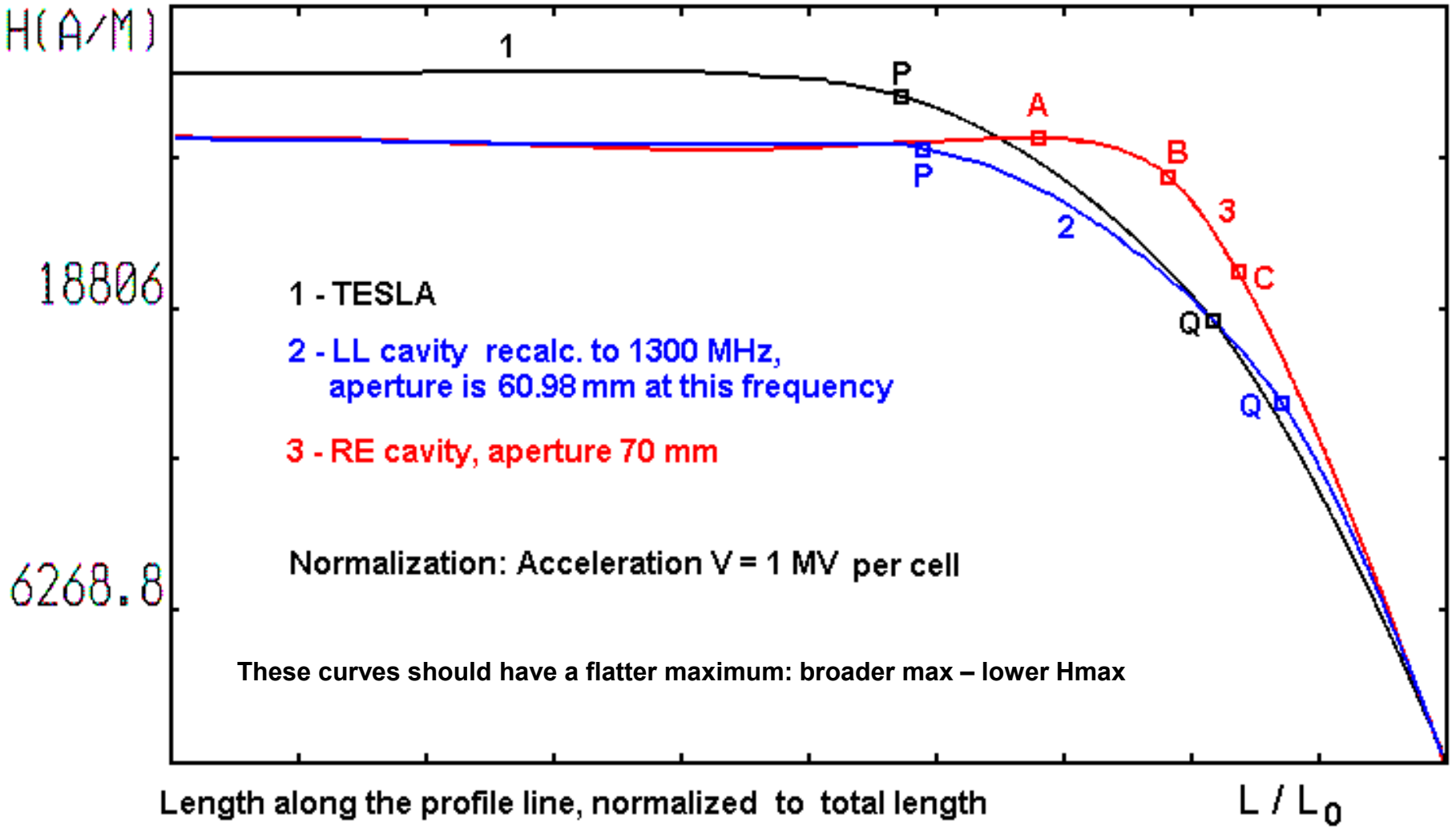

GR/Q for TESLA, LL, and RE cavity

	TESLA	LL	RE	RE	RE
R_a	70	60.98*	70	70	60
E_{pk}/E_{acc}	2.0	2.22	2.0	2.2	2.0
*GR/Q***	1	1.175	1.042	1.081	1.205
$\alpha°$	103	98	81.55	72.93	75.75

*recalculated to 1300 MHz (actually 1500)

**normalized to TESLA: *GR/Q* = 30800 Ohm^2

Some references

- V. Shemelin, H. Padamsee. LNS Report SRF 020128-01, 2002,
  TESLA Report 2002-1,
  Nuclear Instruments and Methods A 496, January 2003.
- In these 3 publications: hard limit of Hpk, means to develop new shapes to reduce Hpk, even if we have to increase Epk, try not to reduce aperture,
- the Reentrant shape design was proposed with minimal value of Hpk/Eacc for any value of Epk/Eacc.
- K. Saito, SRF 2003:
  Since the Hsh (superheating) is ~1800 Gs, if one hopes Eacc = 50 MV/m, …he has to make new cavity design with a small ratio of Hpk/Eacc, for example 36 Gs/(MV/m). Fortunately, we have such a cavity design by J. Sekutovicz et al in JLab [PAC 2003].
- F. Furuta, K. Saito et al. EPAC 2006:
  A thesis of the fundamental limit was proposed by K. Saito [SRF 2003]. He proposed to use a new cavity design with a lower Hpk/Eacc ratio, then still ~50 MV/m would be possible even under the magnetic RF limitation [1st ILC Workshop, 2004].
- K. Saito, 8/17/2006 (from answer to my perplexity request):
  …You have realized the RF cavity design with such a small Hp/Eacc... I agree with you that you have originality in Re-entrant cavity design…

Record results with reentrant cavities

- The first two 1300 MHz single-cell reentrant cavities designed and built at Cornell, have a 70 mm aperture. The ratio of Hpk/Eacc is 10 % lower than that of the TESLA-shape.

  One of them processed and tested at Cornell, achieved a record gradient of 47 MV/m in 2004 [R.L. Geng et al. PAC 2005]

  Another one was sent to KEK for processing and testing and achieved a record gradient of 52 MV/m in 2005 [F. Furuta et al. EPAC 2006]

- The new reentrant single-cell 1300 MHz cavity has a 60 mm aperture. The ratio of Hpk/Eacc is 15 % lower than that of the TESLA shape.

  A record gradient of 59 MV/m was achieved.

  The peak surface magnetic field reached also a record value of 2065 Oe. It has been demonstrated that the reentrant cavity can be pumped down in the presence of trapped water and doesn't show field emission at a peak surface electric field of the order of 100 MV/m [R.L. Geng, PAC 2007]

Left: 60 mm aperture reentrant cavity;
Right: 70 mm aperture TESLA cavity.

70 mm aperture RE cavity test

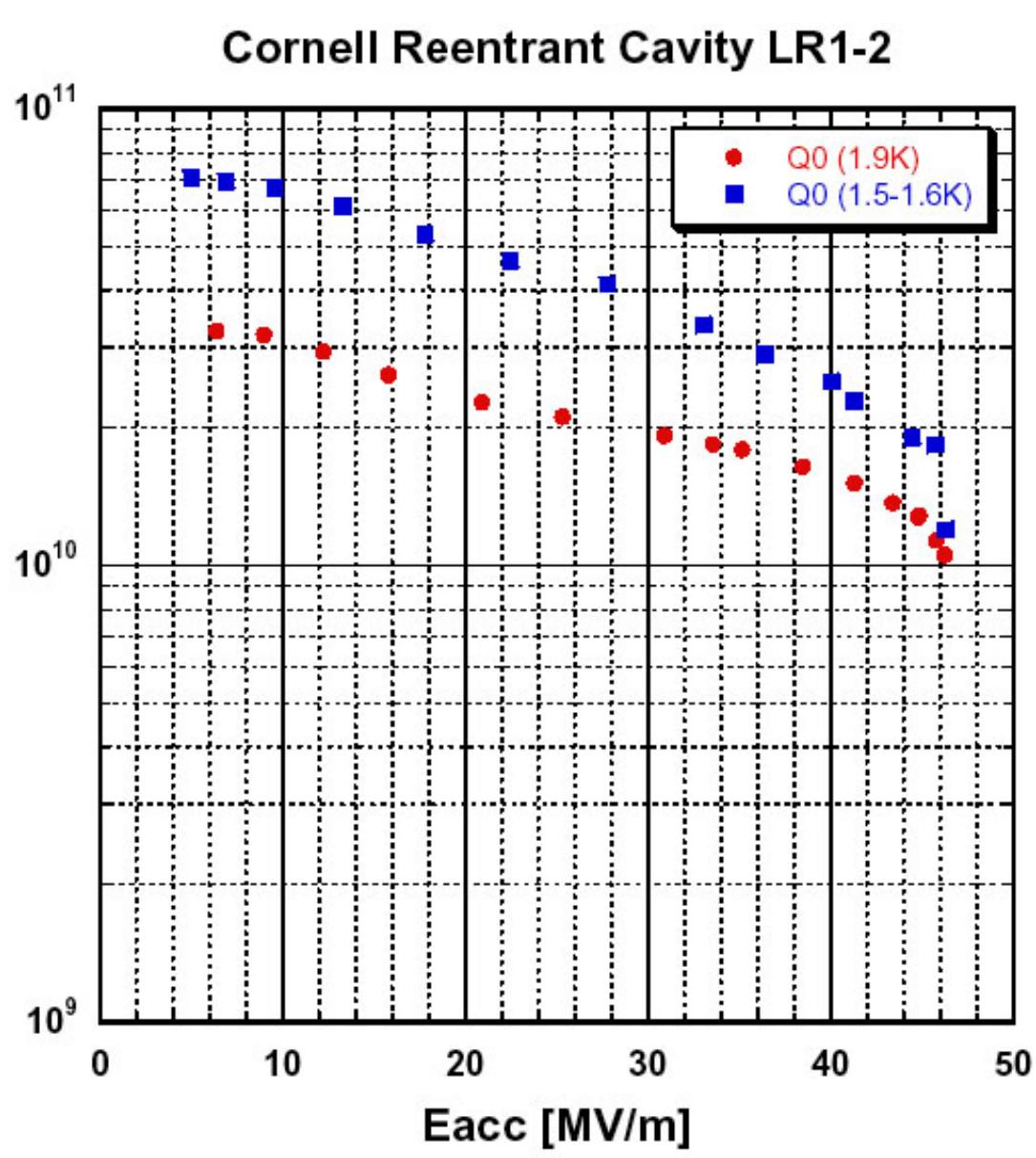

Collaboration with KEK

- **Re-entrant Shape Single Cell Cavity Reached 47 MV/m in May 05**
- **2nd Re-entrant Cavity (built at Cornell) Treated and Tested at KEK Reached 50+ MV/m at KEK (Sept 05)**

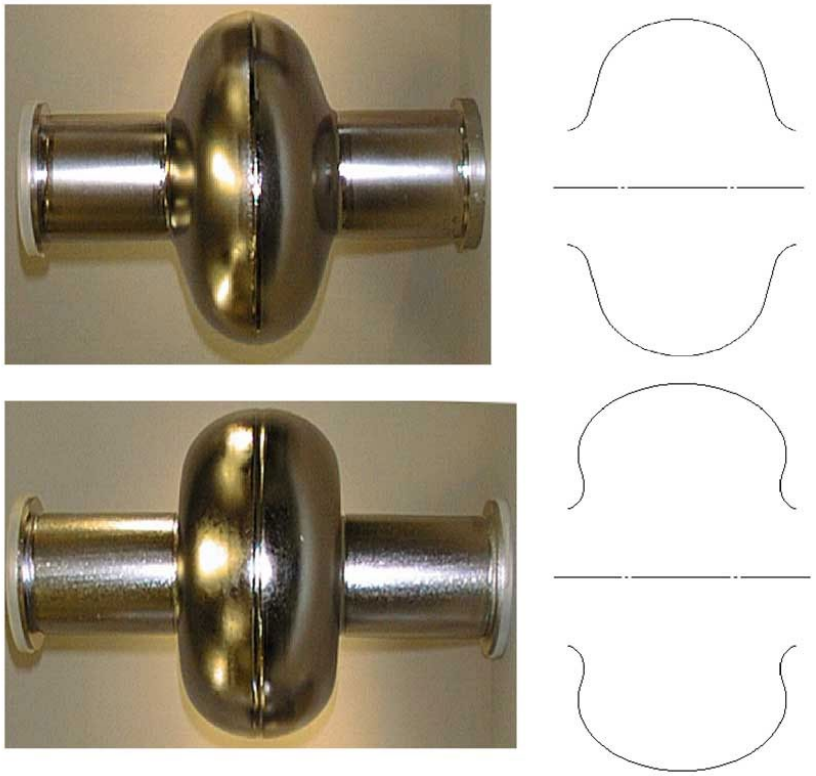

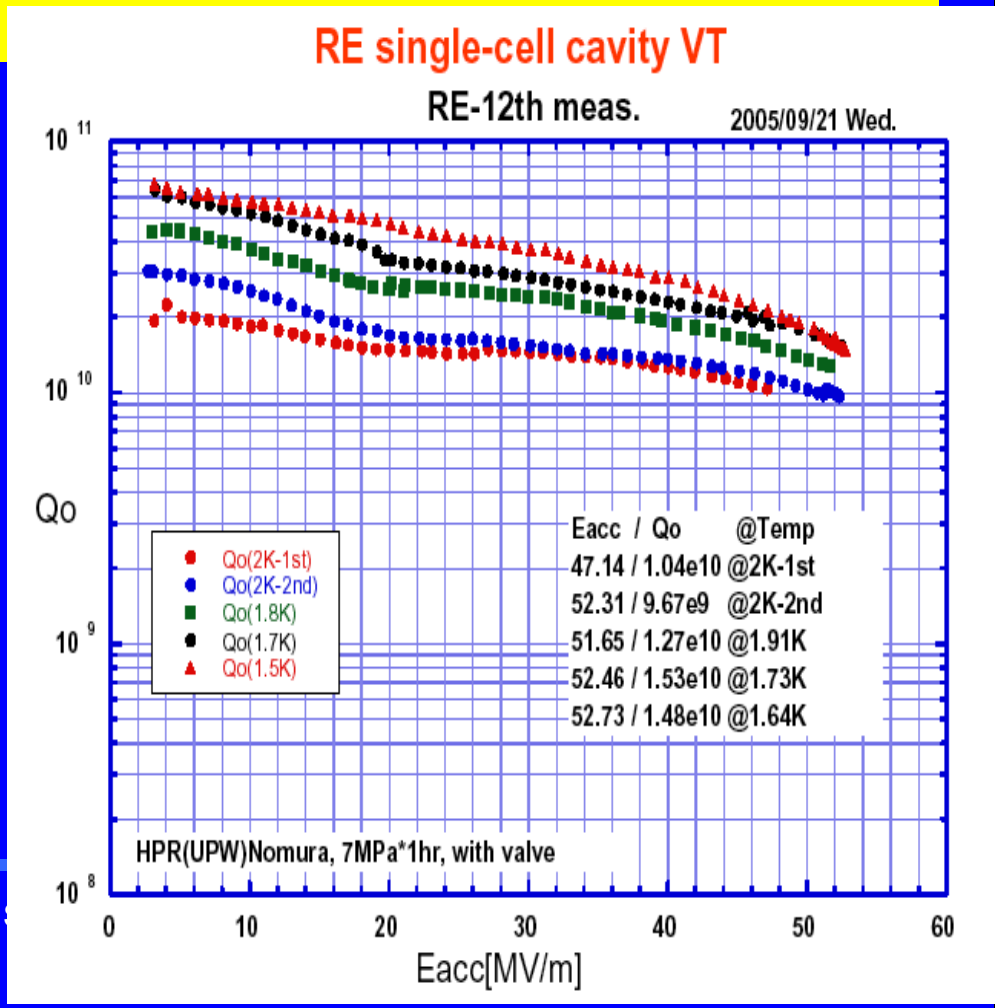

Cornell 60 mm aperture RE cavity test

RE-LR1-3

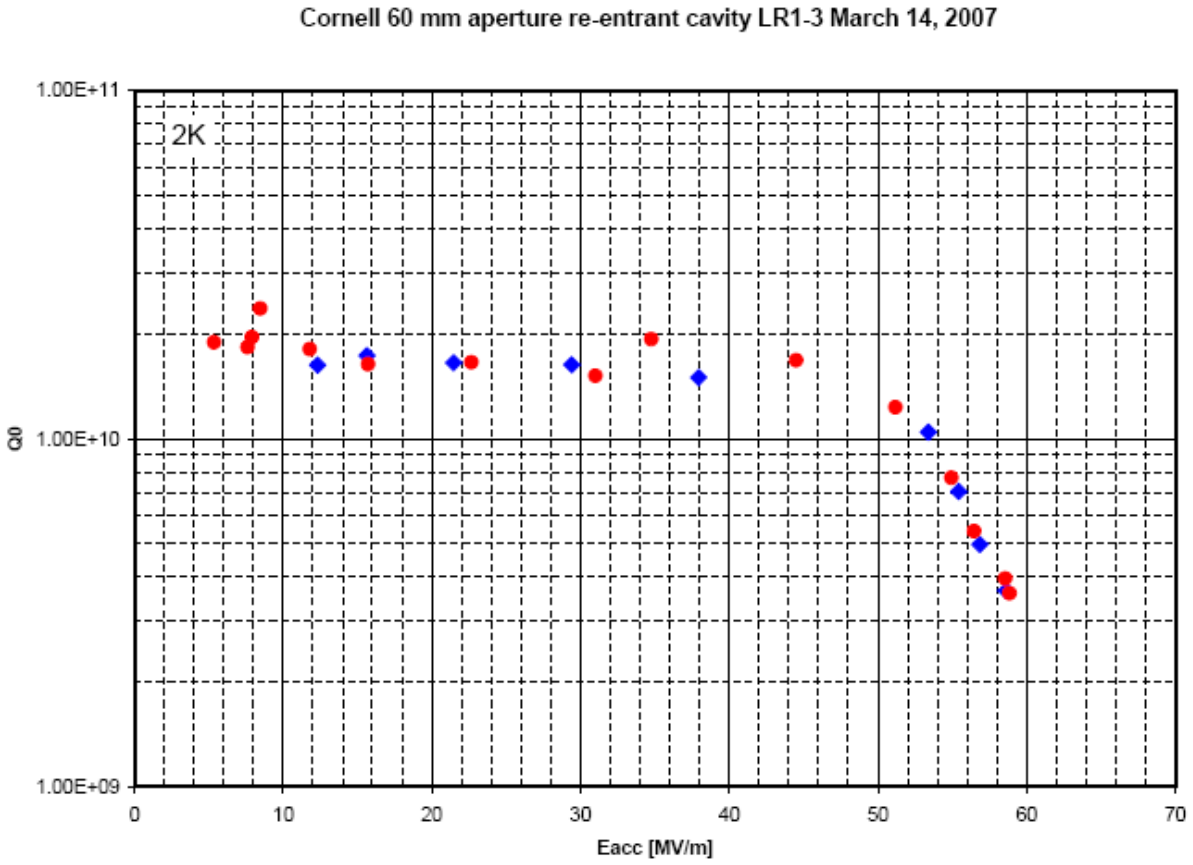

2 items which seem to you clear but … maybe you are wrong (item 1)

- We choose a cavity with 10 % less *H*pk/*E*acc sacrificing 20 % of electric field…
- But we will try to work with the same magnetic field as we did before with the not optimized cavity, to increase *E*acc. In this case we will have the electric field 33 % higher than in the initial situation.

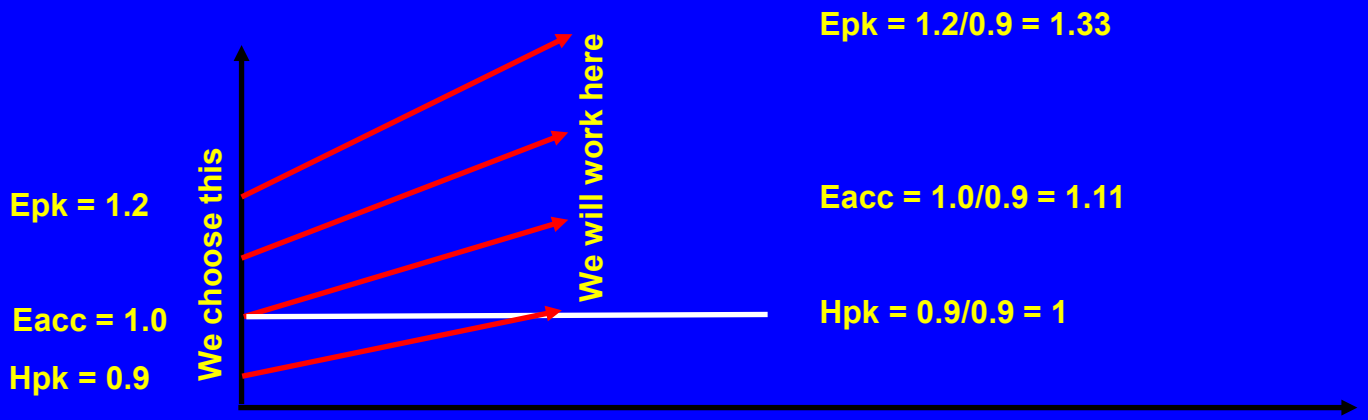

This is a small (inadvertent) lie # 1, about the sacrificed electric field

Be Careful About Single Cell

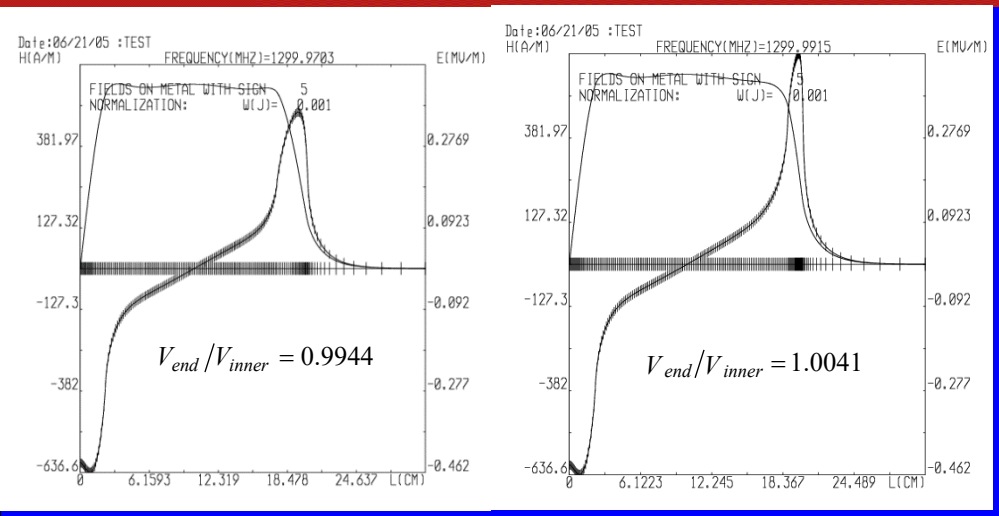

Electric fields along the profile line before (left) and after optimization

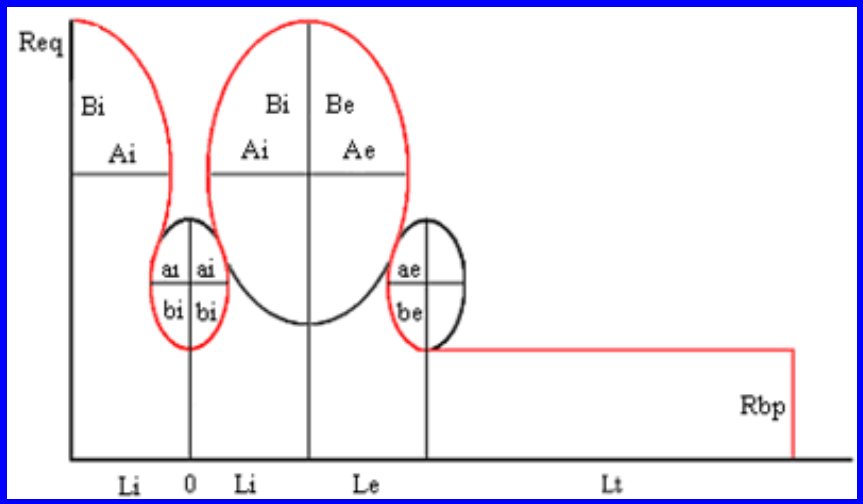

Dimensions of the end cell with Ra = Rbp (aperture radius = beam-pipe radius)

Electric fields in the inner cell are symmetric near the point 0 (lower graph), while in the pipe the field spreads along the pipe and is smaller than the field on the iris (left upper). We can increase the field on the pipe rounding and increase the voltage on the cell (right upper).

But when we compare the one-cell cavity with the multicell cavity – not changing the geometry of the cell - we have benefits for the one-cell: magnetic field is nearly the same but electric field is noticeably less.

For example, for the Reentrant cavity we have:

Design	Iris diam	Hpk/Eacc	Epk/Eacc
Multi-cell	70 mm	37.8	2.40
Single-cell	70	37.9	2.19
Multi-cell	60	35.4	2.28
Single-cell	60	35.2	2.11

This is a small lie # 2, about the single-cell tests

h = *H*pk/*E*acc/42 vs wall slope angle

How fast do the properties of the cell change when the slope angle changes?

To answer this question we need to compare cells with given angle optimized with the same approach as was done without angle limitation and led to reentrant shapes.

RE shapes are left-hand limit points on these graphs

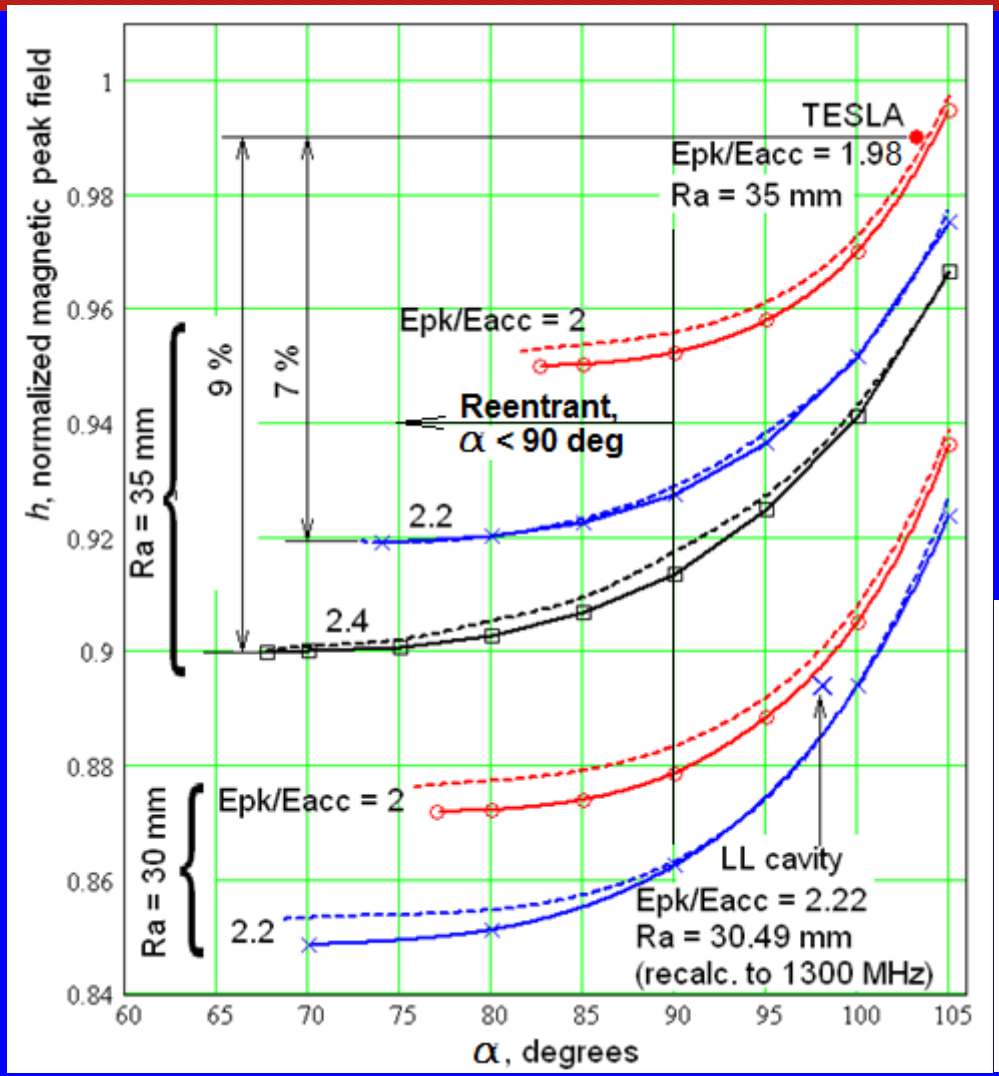

Solid lines present optimization for min *h*, dash lines are results of optimization for max *GR/Q*

Let us remind that the record accelerating field obtained in the reentrant cavity [7] was achieved due to a 9 % lower magnetic peak field at the same compared to the TESLA geometry, though the value of Epk/Eacc was 20 % higher. An attentive analysis of this **Figure** shows that the decrease of *h* by 9 % is by 4 % due to the change of Epk/Eacc from 2 to 2.4 and only by 5 % due to the reentrant shape, i.e. change of the wall slope angle α. Nevertheless, the idea of the reentrant shape for the SRF cavities became well known in the accelerating community.

Can we more increase Ep/Eacc?

GR/Q/30800 vs wall slope angle

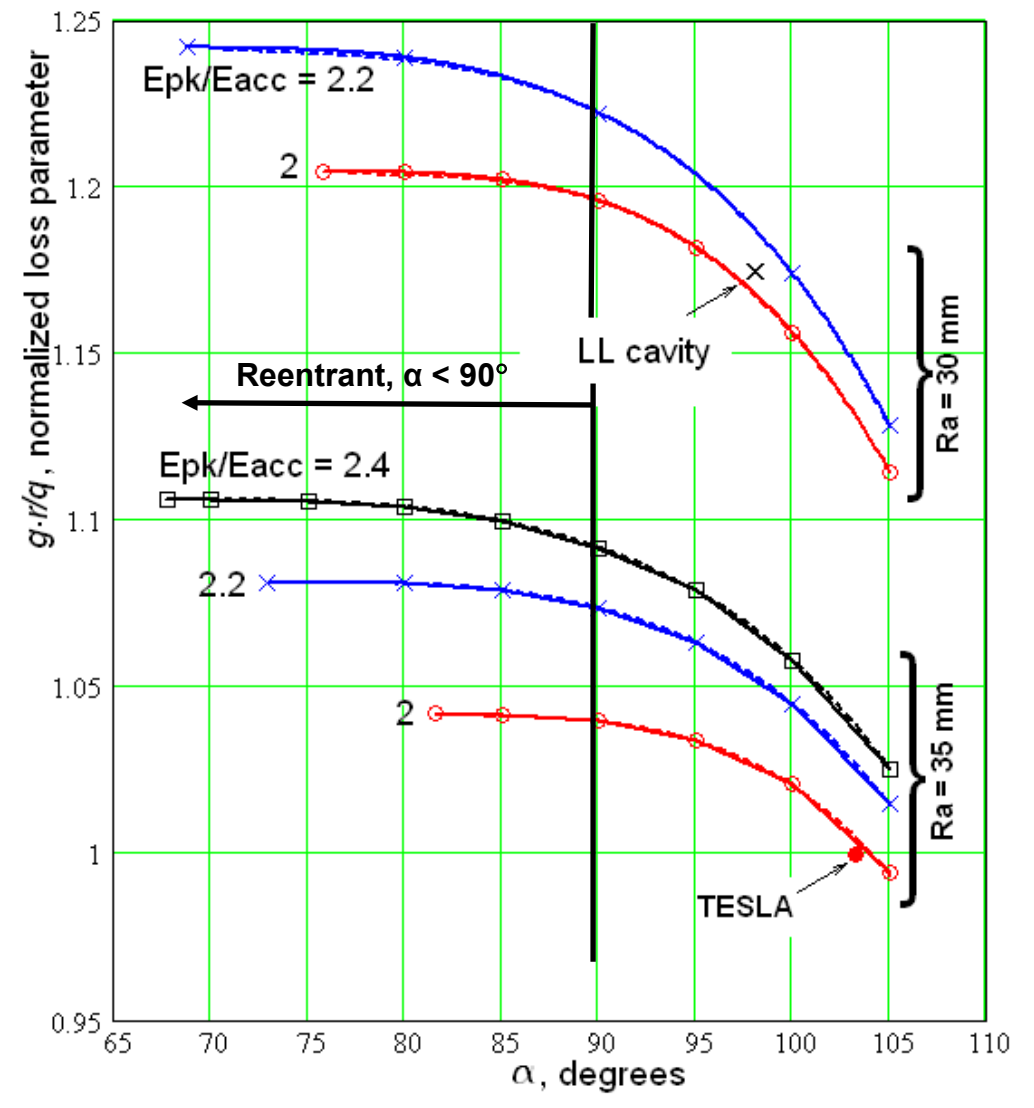

Solid lines present optimization for min *h*, dash lines are results of optimization for max *GR/Q*

But … do you see difference?

When optimizing for max *GR/Q*, the values of *h* slightly increase (max about 0.5 %, previous slide).
When you optimize for lowest *h*, the value of *GR/Q* changes less than 0.1 % from its best value and is on the level of computation error (this graph).

Important result

- There is nothing special in these shapes: TESLA, LL-cavity, ICHIRO-cavity by KEK. All depends on what values of *R*a, *E*pk/*E*acc, and slope angle *α* you can afford or you like. After this you can find your cavity on these curves if it was optimized properly.

- So, it doesn't make sense to distinguish between low losses and high gradient cells. It is the same because both are defined by minimal *H*pk/*E*acc. And this is valid for any slope angle with accuracy better than 0.5 %.

Parameters of elliptic arcs, straight segment lengths, and equatorial radius *vs* angle

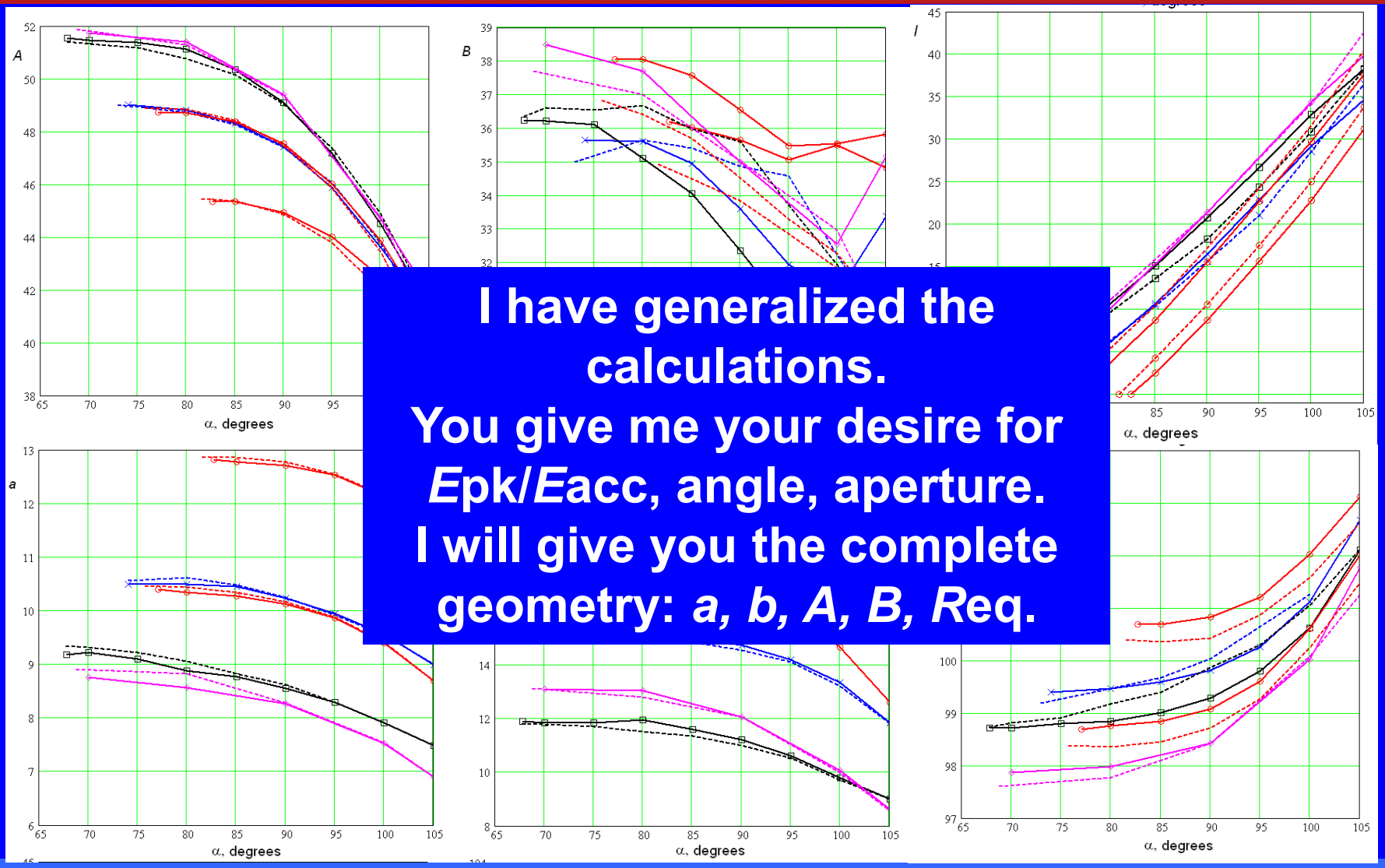

I have generalized the calculations.
You give me your desire for *E*pk/*E*acc, angle, aperture.
I will give you the complete geometry: *a, b, A, B, R*eq.

Case of the reentrant cavity: a 6-arc curve

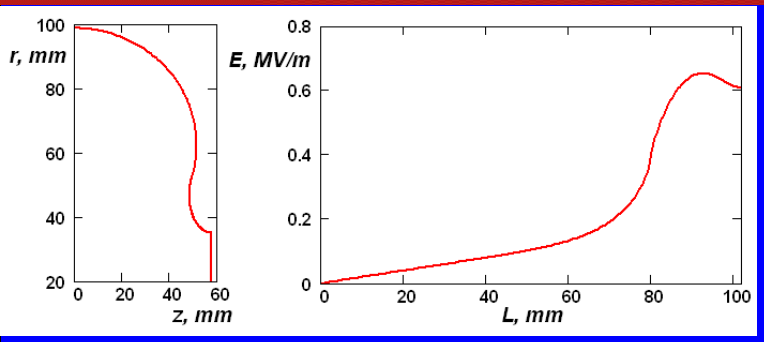

The reentrant cell with 20 % higher electric field and 10 % lower magnetic field than in TESLA cell, shape and electric field along the profile line.

Changing the end 2 arcs of the iris, the *E* field was made flat and 2.4 % smaller *E*pk/*E*acc obtained.

***E*acc does not change.**

There are convenient points to divide the 2-elliptic curve to a 6-circle-arcs curve.

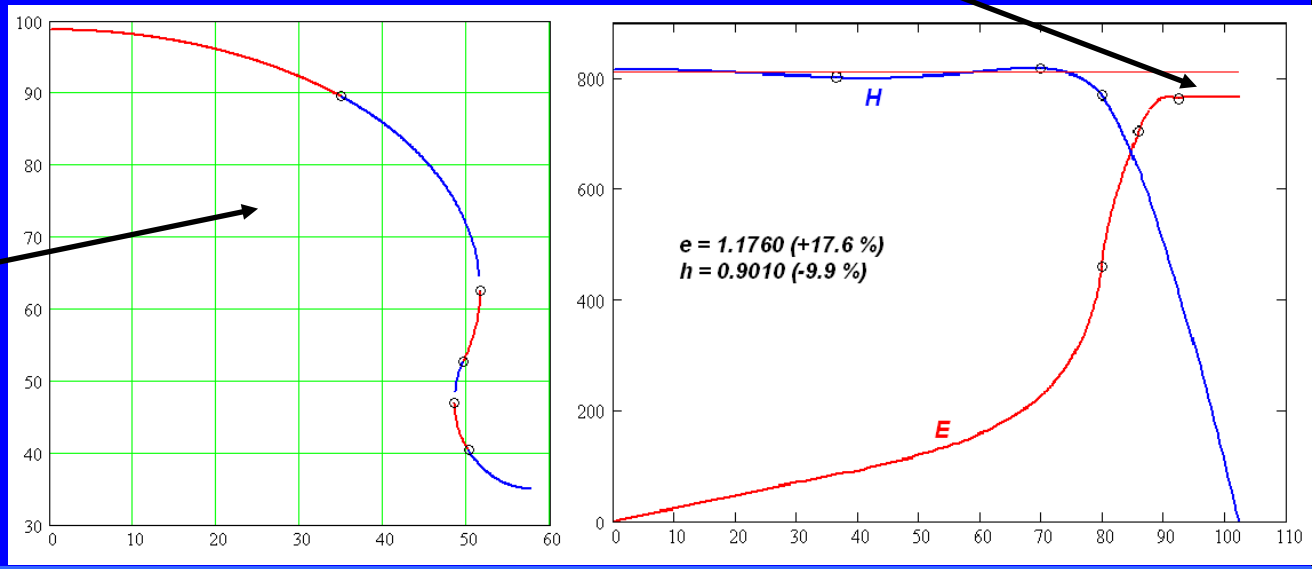

However, I could not make a perfectly flat H-field profile…

More Work for Future
Include Inner and End cells

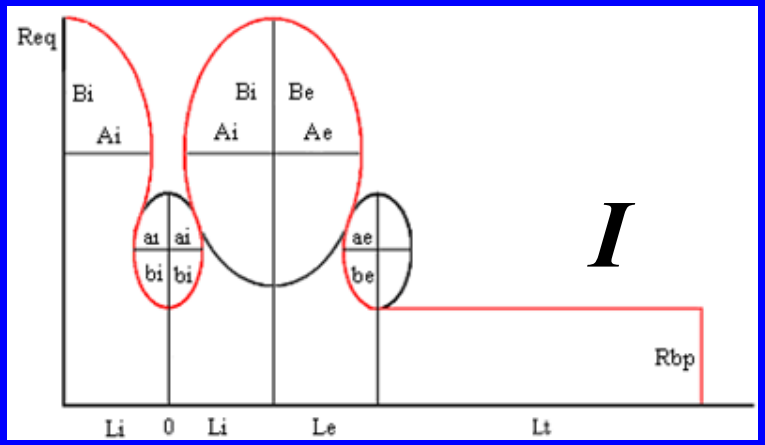

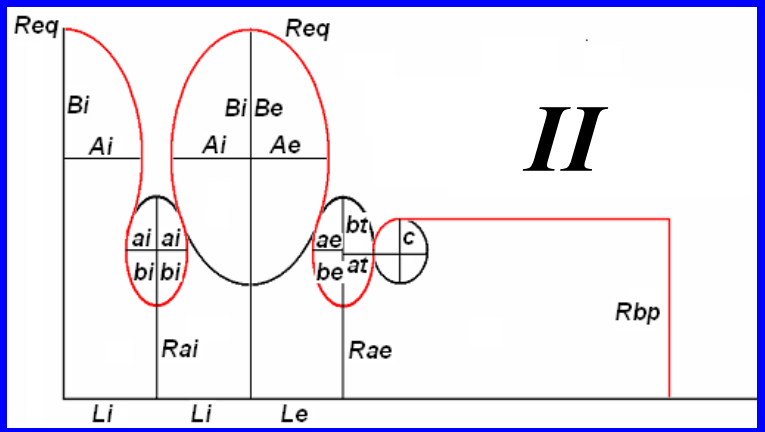

- End cell optimization needs more thought because beam pipe can be larger or equal
- Larger beam pipe helps HOM propagation
- We need to do field profile tuning and *H*pk optimization
  - The length *Le* of the end half-cell is different from *Li* and can be used for tuning the end cell for frequency.
  - If you add the end half-cell to the inner half-cell with the same frequency, the frequency of the result end cell will be different from the initial ones. This is why the end group should be optimized as a whole end cell (with a pipe, what is more), unlike the inner half-cell.
- As already noted, the *E* field distribution along the profile line is such that the curvature of the end cell iris can be made higher, increasing *V*acc of this cell.
- Elliptic shape can be kept for the version *II* with a broader beam pipe for better propagation of the HOMs. For the shape of the ERL injector cavity both, *I* and *II*, versions are used (but not reentrant).
- Shapes *I* and *II* can be optimized using TunedCellEnd, see further.

Results of the other work

$$R(L) = R_{eq} \cdot \frac{h(0)}{h(L)} \cdot \exp\left[-\omega\varepsilon_0 \int_0^L \frac{e(s)}{h(s)} ds\right],$$

$$Z(L) = \int_0^L \sqrt{1 - (dR(s)/ds)^2} ds.$$

Proceedings of IPAC2012, New Orleans, Louisiana, USA. August 19 – 24.

FIRST-PRINCIPLE APPROACH FOR OPTIMIZATION OF CAVITY SHAPE FOR HIGH GRADIENT AND LOW LOSS

Valery D. Shemelin , Georg H. Hoffstaetter

Here, we presented E_s and H_s as functions of the coordinate along the profile line:

$$E_s = e(s), \quad H_s = h(s).$$

If fields along the profile line are known, the shape of the surface can be found with these formulas.

They can be easily checked with the pill-box or the spherical cavity for which the fields can be analytically found.

However, for the arbitrary field distribution the shape can not exist because it should be self consistent.

Equidistant optimization

Optimization of an elliptical cavity is usually done as a search for minimum B_{pk}/E_{acc} when the value of E_{pk}/E_{acc} is given. It is also possible to minimize E_{pk}/E_{acc} for a given B_{pk}/E_{acc} but the truth is that we need to reach as high of an accelerating gradient E_{acc} as possible before field emission or magnetic quench limits E_{acc} from increasing further. So, the ideal situation would be to reach both limits simultaneously using all the possibilities to increase E_{acc}. If we know the maximal achievable surface peak fields E^*_{pk} and B^*_{pk}, then the cavity having equal values of E_{pk}/E^*_{pk} and B_{pk}/B^*_{pk} will be at equal distances from either limit.

New criterion of the shape optimization

Then the criterion of the shape optimization can be written as a minimum of the maximum of two values: E_{pk}/E^*_{pk} and B_{pk}/B^*_{pk}, or, shortly, min max $(E_{pk}/E^*_{pk}, B_{pk}/B^*_{pk})$. We named this approach *the equidistant optimization*.

The definition given above can be rewritten in an equivalent form more convenient for calculations:

$$\text{Goal} = \min E_{pk} \text{ if } E_{pk}/B_{pk} > E^*_{pk}/B^*_{pk} \quad \text{or}$$
$$\text{Goal} = \min B_{pk} \text{ if } E_{pk}/B_{pk} < E^*_{pk}/B^*_{pk},$$

where the Goal is a combination of the geometrical parameters *A, B, a*, and *b*, giving the desired minimum.

Maximal achievable accelerating rates

For example, well optimized for a given aperture, the TESLA cavity has E_{pk}/E_{acc} = 2 and B_{pk}/E_{acc} = 4.2 mT/(MV/m). If we assume that both limits, E_{pk} and B_{pk}, are achieved simultaneously in this optimization, then $E_{pk}/B_{pk} = E^*_{pk}/B^*_{pk}$ = 2/4.2 (MV/m)/mT = 100/210 (MV/m)/mT

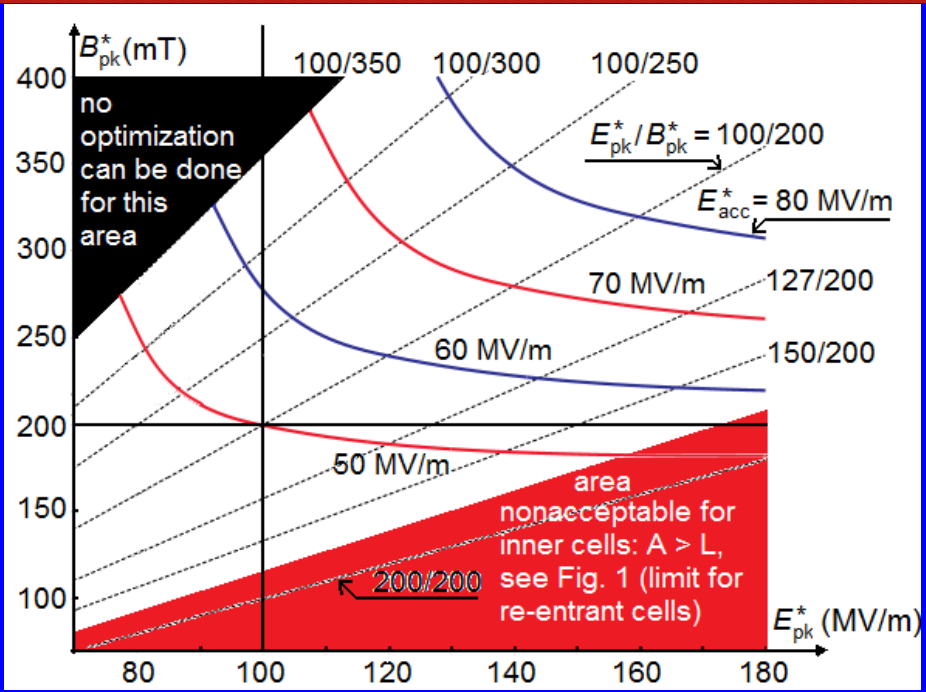

For E^*_{pk} = 125 MV/m that can be achieved now with very thorough surface preparation and with B^*_{pk} = 400 mT that hopefully can be obtained with a new material, we can recon not more than on 80 MV/m. Further increase of the limiting magnetic field B^*_{pk} above 400 mT will not lead to any increase of the accelerating rate as long as E^*_{pk} remains equal to 125 MV/m.

Maximal achievable accelerating rates for different limiting electric and magnetic fields. R_a = 35 mm.

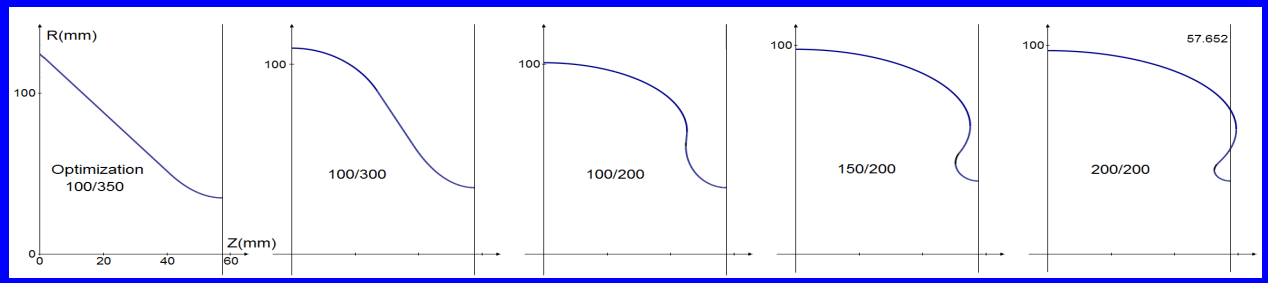

Optimal shapes of inner cells for different values of E^*_{pk}/B^*_{pk}.

HIGH-Q CAVITIES FOR INDUSTRIAL LINACS

Now an industrial linac is under consideration, which is based on Nb_3Sn-coated ILC-type 1.3 GHz acceleration cavity [R. Kephart *et al.*, in *Proc. SRF'15*, 2015], [S. Posen *et al.*, Supercond. Sci. Technol., **34**, p. 025007, 2021].

Lower frequencies are also being considered for industrial linacs: 750 MHz [10], or 650 MHz [11, 12].

[10] G. Ciovati *et al.*, Phys. Rev. Accel. Beams, **21**, p. 091601, 2018.

[11] R. C. Dhuley *et al.*, Supercond. Sci. Technol., **33**, p. 06LT01, 2020.

[12] R.C. Dhuley *et al.*, Phys. Rev. Accel. Beams, **25**, p. 041601, 2022.

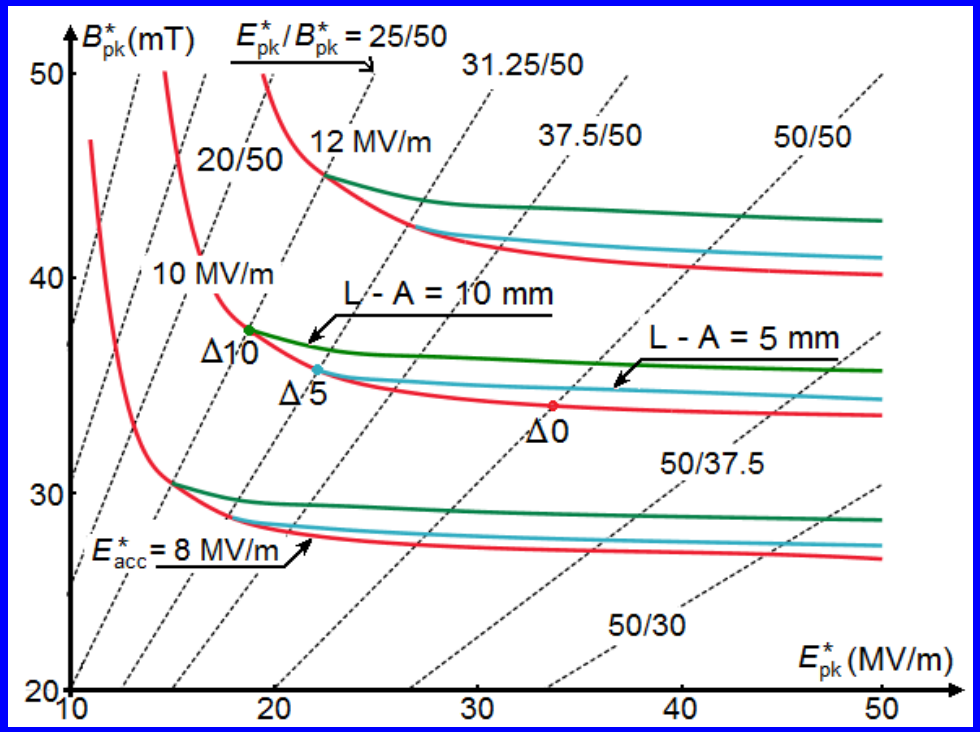

An increase in gradient have been demonstrated with cryocoolers at a frequency of 915 MHz, up to 12.8 ÷ 13.6 MV/m [13], but it was done with a single-cell cavity whose optimization is different, and for a low β, the speed of the electron relative to the speed of light.

G. Ciovati *et al.*, Phys. Rev. Accel. Beams, **26**, p. 044701, 2023.

Equidistant optimization for inner cells of a multicell cavity when the increase of A is limited by certain values. Aperture radius R_a = 30 mm.

The found best shapes can decrease losses up to 30 % compared to commonly used (ILC-type) cavities at the same accelerating rate.

Conclusions for Shape

- 3 parameters can be chosen for a cell as "primary parameters": aperture radius, *E*pk/*E*acc, and wall slope angle. After this you can find the best two-elliptic shape: with min losses and min *H*pk/*E*acc, from the results presented here.
- The shape with min *H*pk/*E*acc is the best from the viewpoint of losses too, within errors of fabrication, for any wall slope angles, apertures, and *E*pk/*E*acc.
- Optimization of end cells depends on the chosen transition to the beam-pipe, and has more parameters to be defined.
- Some small improvement of the existing RE (and non-RE) shape is possible, several %% (5%?) in *E*pk or (and) *H*pk if we go out of the elliptic shape paradigm.

  However, the ILC accelerating structure will cost of the order of $1B, and even 1 % of $1B is $10M, that is much more than expenses needed for this improvement. So, it should be done.

The new approach, Equidistant Optimization, reveals the physical meaning of the chosen Epk/Eacc, makes possible to predict the maximal possible accelerating gradient for different limiting fields, specifically for high or low magnetic field, and leads to the best shape for any chosen limitations, not fields only but also for wall inclination, aperture radius, width of a cell etc.

SLANS family of codes

SuperLANS (or SLANS) is designed to calculate monopole modes of axially symmetric RF cavities using a finite element method of calculation and a mesh with quadrilateral bi-quadratic elements (see Fig).

SLANS calculates the mode frequency and many secondary parameters such as the quality factor, stored energy, transit time factor, geometric shunt impedance, maximal electric and magnetic fields, acceleration, acceleration rate. The program interface allows plotting for a given mode its field distribution along axis, force lines, and surface fields. All fields can be written into output file in ASCI format.

Input data for SLANS present a table (see insert in Fig.) describing the boundary of a cavity geometry. The boundary may consist of straight segments and elliptic arcs. If the cavity is symmetric, only one half of its geometry may be entered while specifying a boundary condition at the plane of symmetry. This boundary condition can be either “electric wall” or “magnetic wall”. SLANS also allows including lossless dielectric materials into the cavity geometry.

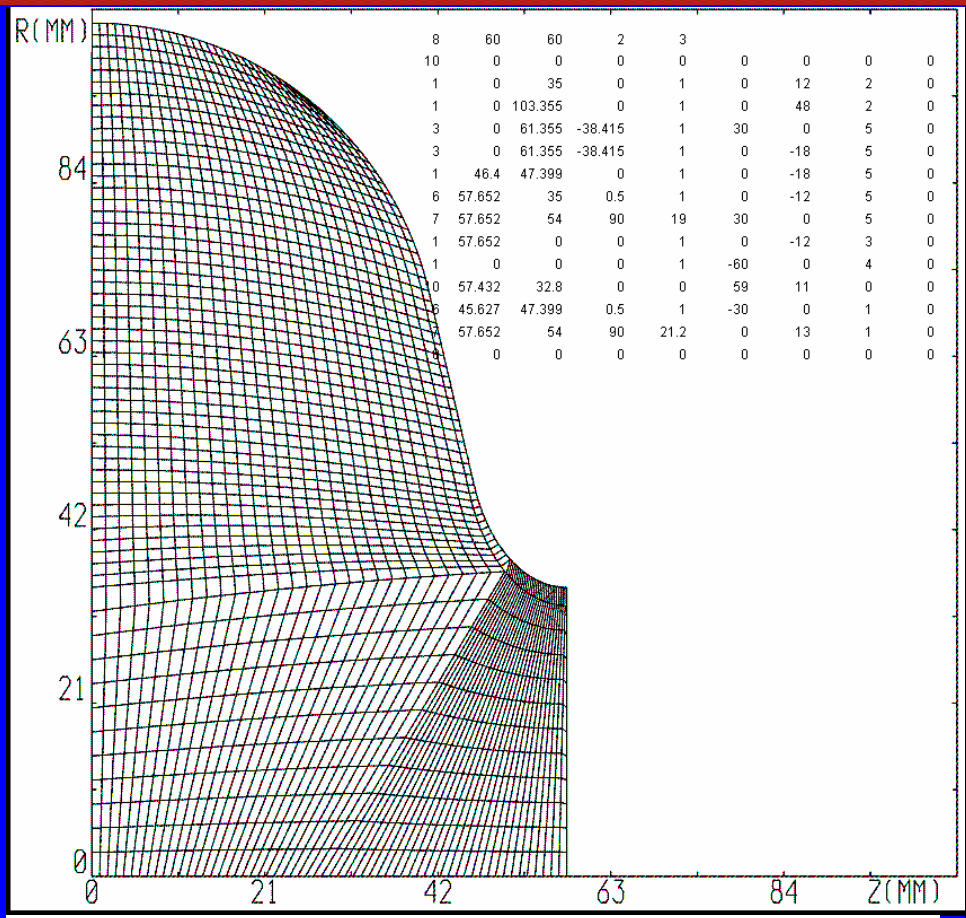

There are more codes belonging to the SLANS family. **CLANS s**olves eigenvalue problem for monopole modes in geometries containing lossy dielectric and ferromagnetic insertions. Programs **SLANS2** and **CLANS2** calculate azimuthally asymmetric (dipole, quadrupole, etc.) modes in cavities. The latter program allows including lossy materials.

Spherical cavity: Analytical formulas. Comparison of codes. Sergey Belomestnykh. SRF 941208-13 (Cornell U. site)

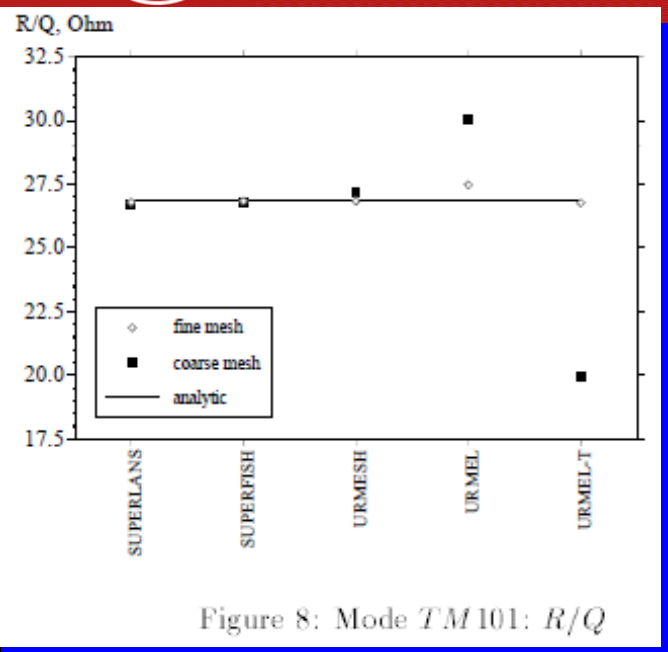

Figure 8: Mode $TM101$: R/Q

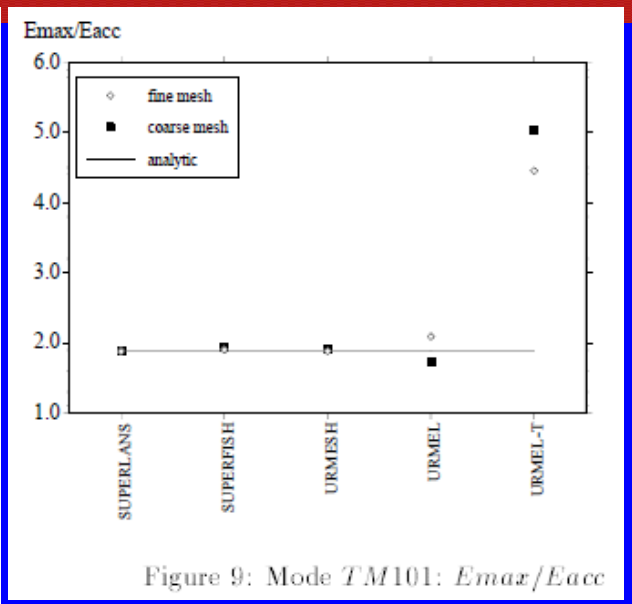

Figure 9: Mode $TM101$: $Emax/Eacc$

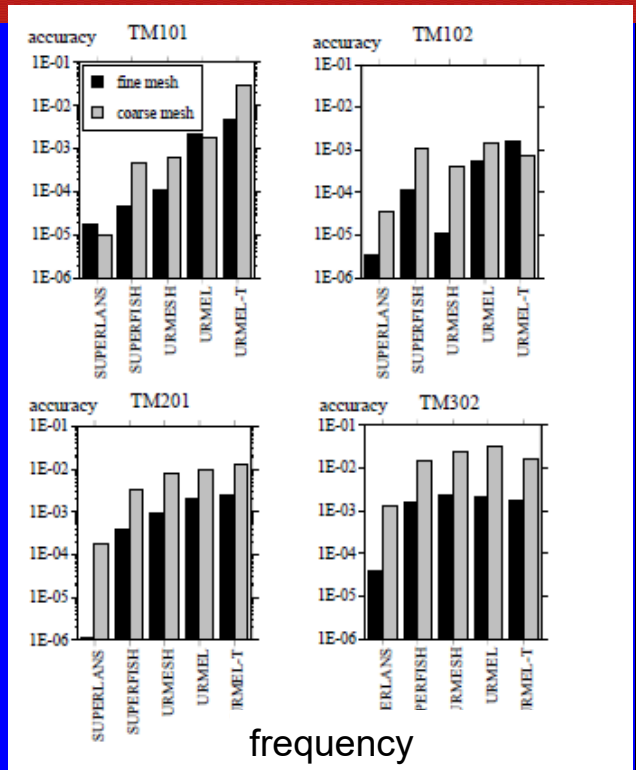

Figure 10: Accuracy for different HOMs

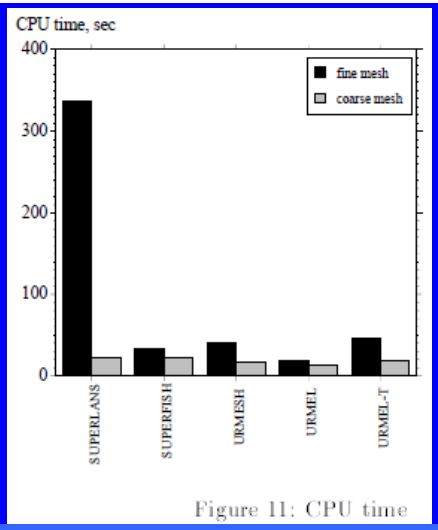

Figure 11: CPU time

Coarse mesh: 10 x 10
Fine mesh: 30 x 30

Work file for TunedCell

tuned.tgp - Notepad

File Edit Format View Help

```
97.873    30    57.6524 : Req(mm), Rbp(mm), L(mm)
1300                1 : Freq(MHz), mode
1.                 16 : delta(mm), m
47.65     46.27     0 : A1(mm), A2(mm), nA
45.14     45.26    12 : B1(mm), B2(mm), nB
14.64     14.76    12 : a1(mm), a2(mm), na
2.64       2.76    12 : b1(mm), b2(mm), nb
0          19.6    -1 : l1(mm), l2(mm), nl
1.e-7      100      3 : delta freq, f_iter, n_l
1        : r - reentrant 1.0 or no - 1.0
28.5  28.5    1 : x_begin x_end(mm), automatic                beta should be given in the dtr file.
```

A	B	a	b	l	Req	Freq	h	rh	zh	e	re	ze	Q	Rsh	ee	he	it	RE	alpha	beta
47.650	45.140	14.640	2.640	4.701	97.873	1300.000	0.842574	72.389	42.895	2.953643	32.525	43.026	28180	2.126294	5.907285	35.388121	3	1	68.861436	1
47.650	45.140	14.640	2.650	4.658	97.874	1300.000	0.842605	72.395	42.893	2.948829	32.535	43.026	28180	2.126127	5.897658	35.389401	4	1	68.818257	1
47.650	45.140	14.640	2.660	4.614	97.875	1300.000	0.842635	72.400	42.891	2.944038	32.545	43.026	28181	2.125960	5.888077	35.390662	4	1	68.774543	1
47.650	45.140	14.640	2.670	4.570	97.876	1300.000	0.842665	72.405	42.888	2.939269	32.554	43.026	28181	2.125794	5.878537	35.391917	5	1	68.730227	1
47.650	45.140	14.640	2.680	4.526	97.877	1300.000	0.842695	72.410	42.886	2.934522	32.564	43.026	28181	2.125627	5.869043	35.393179	5	1	68.685449	1
47.650	45.140	14.640	2.690	4.481	97.878	1300.000	0.842725	72.416	42.884	2.929792	32.574	43.026	28181	2.125461	5.859585	35.394438	5	1	68.640094	1

TunedCell is an envelope file for SLANS. It was created by Dmitry Miakishev on my request. This is an example of the work file for TunedCell. It calculates cell parameters for a set of geometrical data.

You can enter the geometry of the cell, the range of length variation of the axes of elliptic arcs, number of passing points between boundaries of this range, accuracy of calculation.

The program will find the equatorial radius Req, tuning the cavity to a given frequency, maximal surface fields, points where these maxima are reached, shunt impedance and Q-factor (for copper by default but you can enter any conductivity in the .dtr file), angle of inclination for the straight part of the wall.

You can use the .geo file, file of geometry, created by TunedCell for the last line, and work with it using the SLANS alone, which has much more options.

Procedure of optimization

Let us first discuss the search of minimum h = Hpk/Eacc/42 for a given value of e = Epk/Eacc/2.
So, we are going to minimize the function h(A, B, a, b) under given constraints: e should be less or equal to the maximal allowed, and the value of α (angle) should be greater than or equal to the minimal allowed.
The "brute force" or "grid search" is to calculate h on a 4D grid around an initial central point, find the min h between the neighboring points, make the point of min the new central point, and repeat the procedure until the min h is found for a given step size. Then the step can be decreased until we reach the required accuracy. However, a 2D example presented in Figure shows that this method is inefficient when the optimized function belongs to a class of so-called ravine functions. Gradient decent also appeared inefficient.

We exactly have the case of a so-called ravine function: a rapid descent to the boundary and gently declined path along the boundary. In the search of the minimum h, the algorithm quickly comes to the boundary where the limiting values of e and α are reached. To move along the "bottom" of the ravine, we can solve the following system of equations:
$\partial h/\partial A \cdot \Delta A + \partial h/\partial B \cdot \Delta B + \partial h/\partial a \cdot \Delta a + \partial h/\partial b \cdot \Delta b = \Delta h$,
$\partial e/\partial A \cdot \Delta A + \partial e/\partial B \cdot \Delta B + \partial e/\partial a \cdot \Delta a + \partial e/\partial b \cdot \Delta b = \Delta e = 0$,
$\partial \alpha/\partial A \cdot \Delta A + \partial \alpha/\partial B \cdot \Delta B + \partial \alpha/\partial a \cdot \Delta a + \partial \alpha/\partial b \cdot \Delta b = \Delta \alpha = 0$,
where Δh is a negative value to be added to h to decrease it.
The system is underdetermined as we have three equations and four unknowns: ΔA, ΔB, Δa, and Δb.
A fourth equation can be added to define length of the vector of increment, s, so that the system of equations becomes solvable:
$\Delta A^2 + \Delta B^2 + \Delta a^2 + \Delta b^2 = s^2$. For any Δh we can choose s, preferably small.

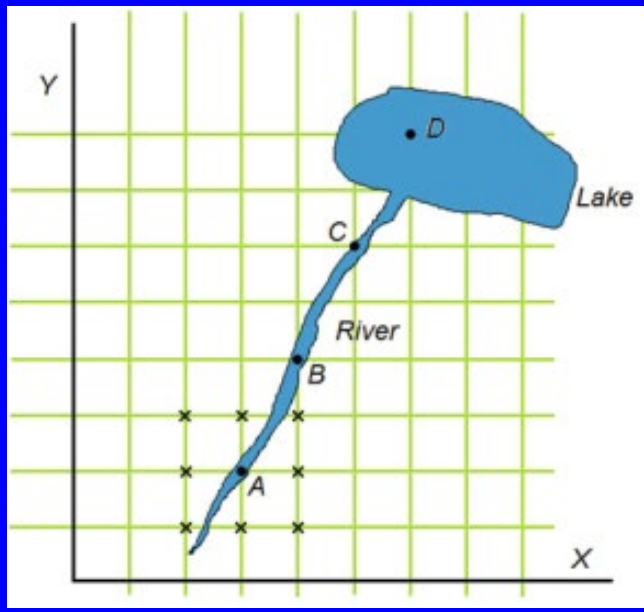

Procedure of optimization (2)

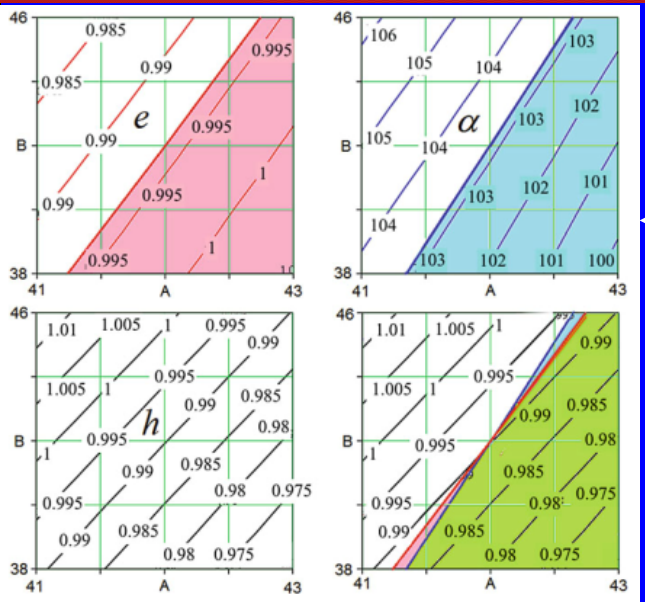

Fig. 10.3 Contour plots for TESLA cavity near the nominal values of A and B. a = 12 mm and b = 19 mm

One can see that on the line h = 0.99 the value of e is almost constant as well. Shifting up and left – h grows, shifting to smaller h, - e grows. So, we can change A and B moving along this line (or this "ravine") practically not changing neither h nor e.

If we want to improve h, not increasing e and not decreasing α, we declare the pink area for e and the blue area for α **as** "forbidden". When we overlap contours for e, h, and α, we can see that h can be improved at the point A = 41.25, B = 38.

Green is "twice forbidden" area.

After further optimization, we come to Fig. 10.4. Here, we slightly deviated from the TESLA geometry by choosing α = 100° (was 103.17 °), and e = 1. Both of these changes improved the value of h, from 0.99 to 0.97 but this is not the main result.

We believe that the main result is the fact that moving along the forbidden area, we can change both A and B in a wide range while changing the value of h no more than 0.5 %. This very shallow minimum gives us a possibility to create a practically optimal cavity geometry free of multipactor.

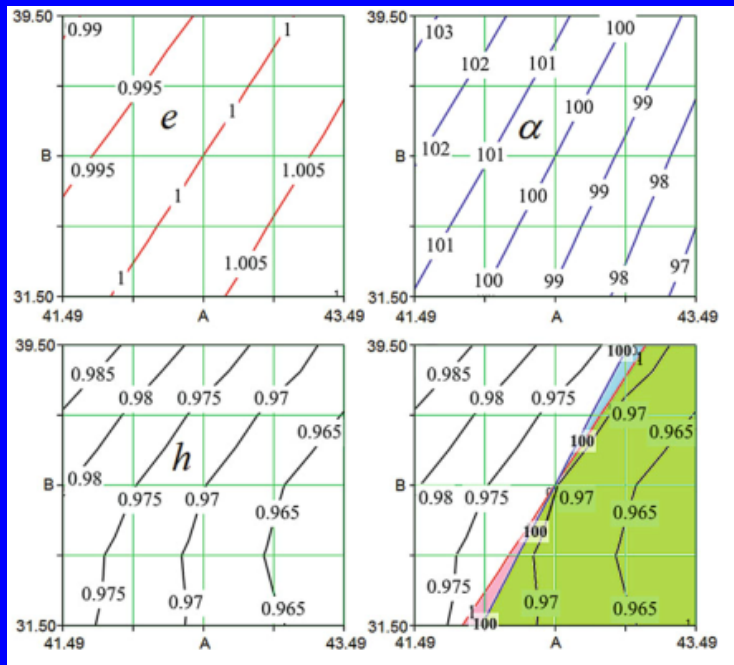

Fig. 10.4 Contour plots for the optimized TESLA cavity with a = 12.13 mm, b = 19.70 mm

Multipactor, 100 years soon

The multipactor effect was first observed by French physicist Camille Gutton 99 years ago, in 1924 and has been studied in subsequent years by him and his son as a discharge in ionized gas.

However, this phenomenon was identified as a secondary emission discharge and further studied, 10 years later, in 1934, by Philo T. Farnsworth, the inventor of electronic television.

A multipactor (or AC Electron Multiplier) first was a device where the electrons make *multiple impacts* on metal electrode surfaces, freeing the secondary electrons.

If there is a high-frequency electric field in the volume of the device, the electron can absorb energy from this field under certain conditions and their number can increase like an avalanche due to secondary emission.

It was one of few attempts “to tame” this phenomenon, (later - ion source by H. Alfvén, electron gun by W. Gallagher and Maury Tigner) but these inventions did not find wide use.

Moreover, nowadays the multipactor effect has become an obstacle to be avoided in normal operation of accelerating structures and RF windows, vacuum electronics, radars, satellite communication devices, etc.

Multipactor. A simple case: flat gap

The equation of motion for an electron in the gap of width *d* is $\ddot{x} = \frac{e}{m}\frac{U}{d}\sin\omega t,$
e is positive for simplicity of writing.

It is helpful to rewrite this in normalized form $\lambda'' = \xi \sin\theta,$ (1)

where $\lambda = x/d, \xi = U/U_0, U_0 = m\omega^2 d^2/e,$ and $\theta = \omega t;$

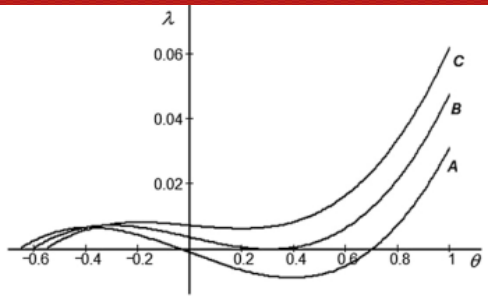

Trajectories of electrons started at negative phases. Some of them will return, see below, line '3'.

Integrating (1), we obtain

$$\lambda' = \xi(\cos\theta_1 - \cos\theta) + \beta_1,$$

$$\lambda = \xi(\theta - \theta_1)\cos\theta_1 + \xi(\sin\theta_1 - \sin\theta) + \beta_1(\theta - \theta_1), \quad (2)$$

The condition for the electron to "resonantly" cross the gap is that the transit time be equal to an odd number of half-periods of the RF field. This ensures that newly generated secondary electrons see the same relative phase of the field as their predecessors. From (2):

$$1 = \xi(\theta_2 - \theta_1)\cos\theta_1 + \xi(\sin\theta_1 - \sin\theta_2) + \beta_1(\theta_2 - \theta_1)$$

$$\xi = \frac{1 - (\theta_2 - \theta_1)\beta_1}{(\theta_2 - \theta_1)\cos\theta_1 + 2\sin\theta_1} = \frac{1 - (2n-1)\pi\beta_1}{(2n-1)\pi\cos\theta_1 + 2\sin\theta_1}$$

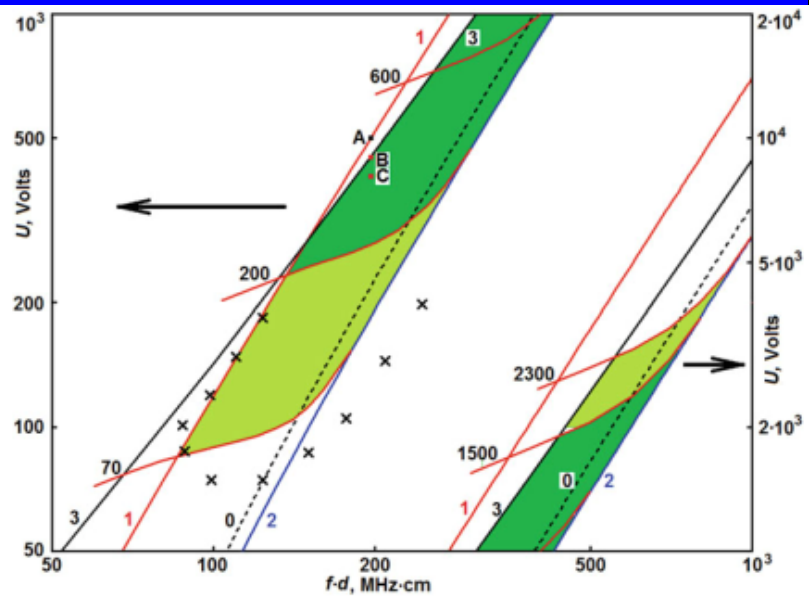

Zone n = 1 for multipactor discharge. '1' and '2' indicate stability bounds. 70, 200, 600 etc. – energy of primary electrons in eV. Energy of secondary electrons is 4 eV.

Bounds of the zones are defined by Secondary Emission Yield and by the Stability Condition

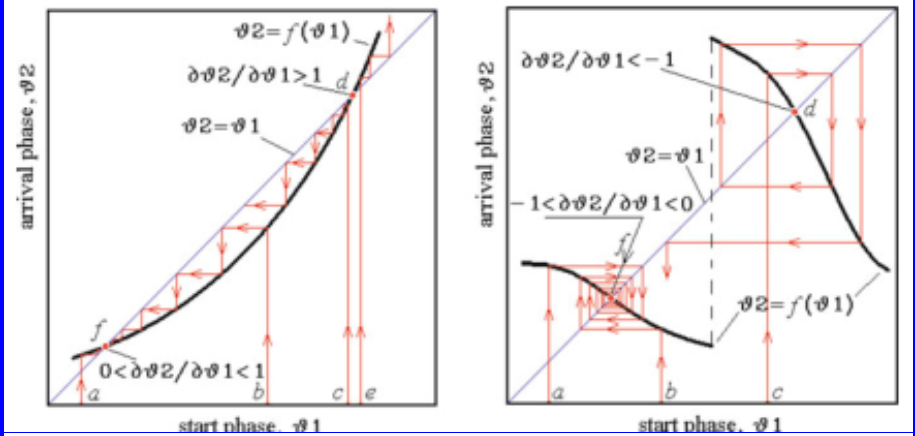

Focusing to a stable phase and defocusing from an unstable phase for an increasing and decreasing function θ2 = *f*(θ1). $|\partial\theta_2/\partial\theta_1| < 1.$

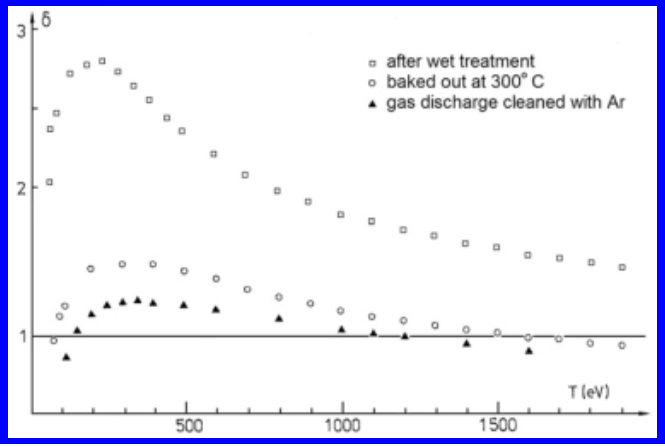

SEY of a niobium surface after different surface treatments as a function of the energy of the impacting electrons

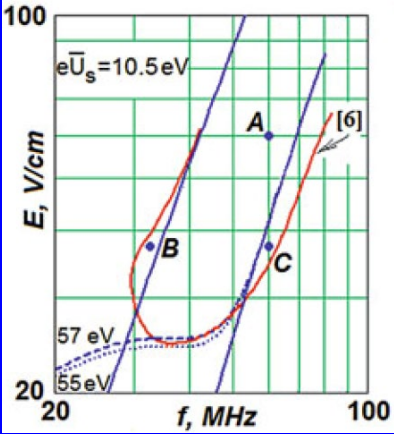

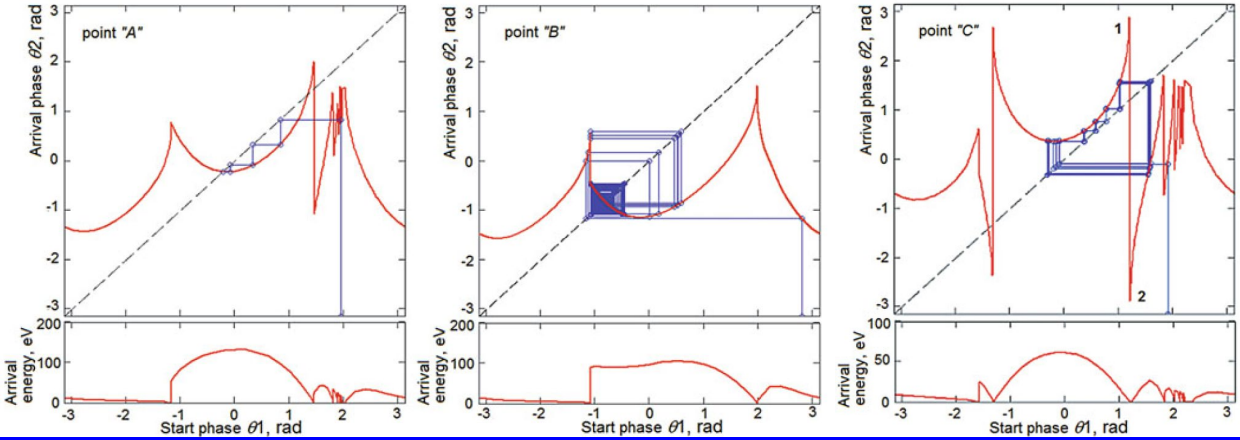

Experimental curve [A. J. Hatch, H. B. Williams, 1954] and generalized stability condition: $\left|\frac{\theta_2^r - \theta_2^l}{\theta_1^r - \theta_1^l}\right| < 1$

Experimental Study with 430 MHz Test Cavity

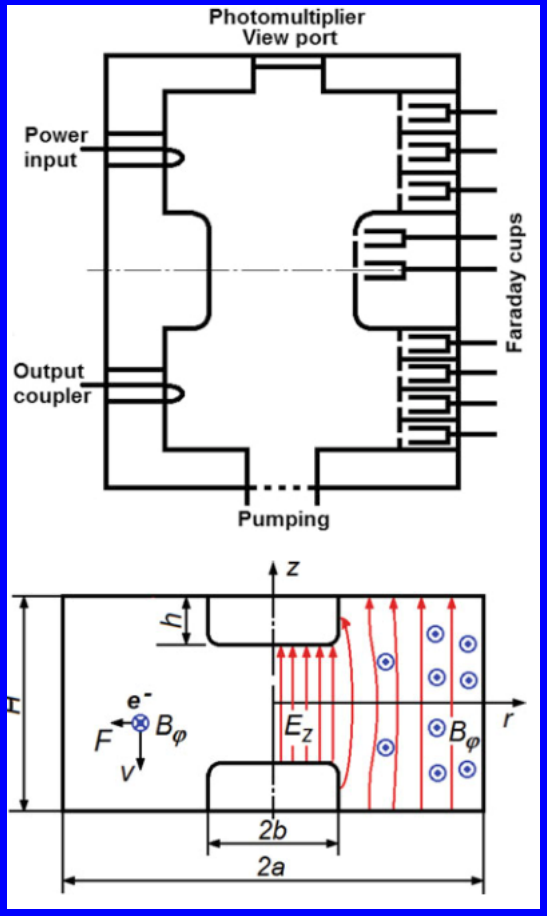

The accelerating gap of the cavity H − 2h = 125 mm, the diameter 2a is 465 mm, the height of the reentrant stubs h is 48 mm, and the diameter of reentrant stubs 2b = 107 mm.

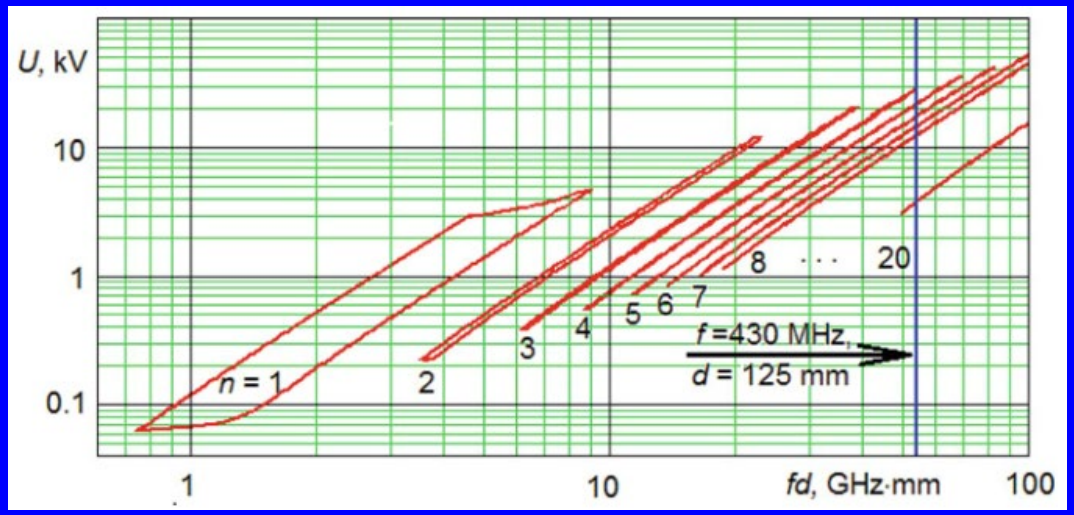

During operation of the storage ring VEPP-3 [3], the voltage on the 72.5 MHz accelerating cavity is slowly varied through a wide range of amplitudes. At some voltage levels, this cavity can be prone to multipacting, which prevents an increase in the voltage.
It was necessary to study multipactor and find a means of suppressing it.
An experimental setup was developed for this purpose. Keeping in mind that multipacting zones depend on *f d* and to ease the handling, a smaller test cavity with the geometry close to the VEPP-3 cavity but scaled to a higher frequency (430 MHz) was built.

Multipactor was observed in the central area of the cavity at voltages on axis Ures from 7 to 50 kV with two maxima, at 12 and 25 kV.

The VEPP-3 electron-positron storage ring. (Budker Institute of Nuclear Physics.) http://v4.inp.nsk.su/vepp3/index.en.html.

Multipactor on the cavity equator

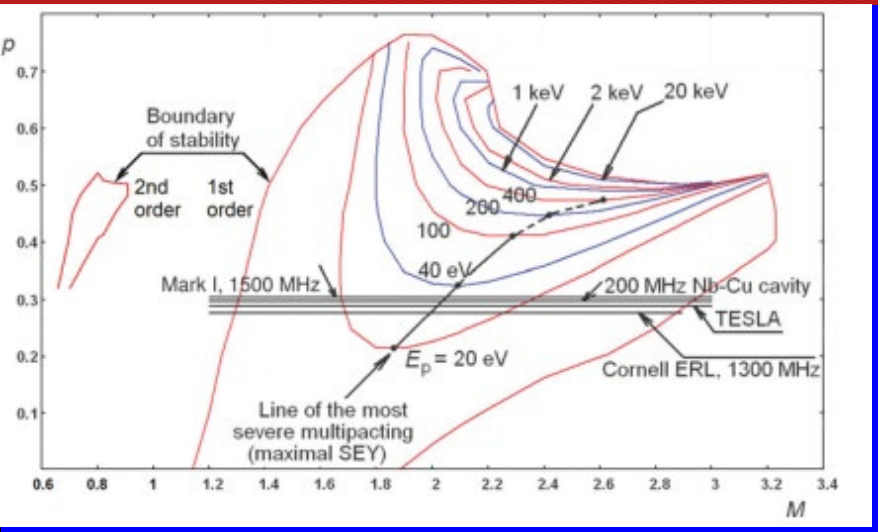

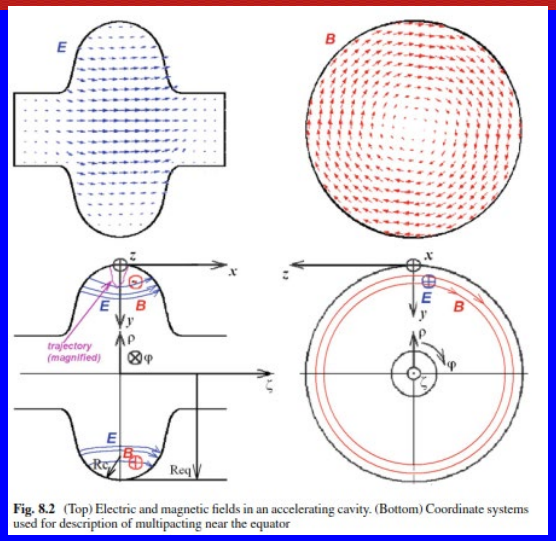

Fig. 8.2 (Top) Electric and magnetic fields in an accelerating cavity. (Bottom) Coordinate systems used for description of multipacting near the equator

$$B_z = -B_0 \cos\theta,$$
$$E_x = \alpha \cdot y \cdot \sin\theta,$$
$$E_y = -\beta \cdot x \cdot \sin\theta.$$

$$e\,(E_x + \dot{y}B_z) = m\ddot{x},$$
$$e\,(E_y - \dot{x}B_z) = m\ddot{y}.$$

$$\dot{x} = \omega x', \quad \ddot{x} = \omega^2 x'', \text{ and so on,}$$

$$x'' = M[(1-p)y\sin\theta - y'\cos\theta],$$
$$y'' = M(-px\sin\theta + x'\cos\theta).$$

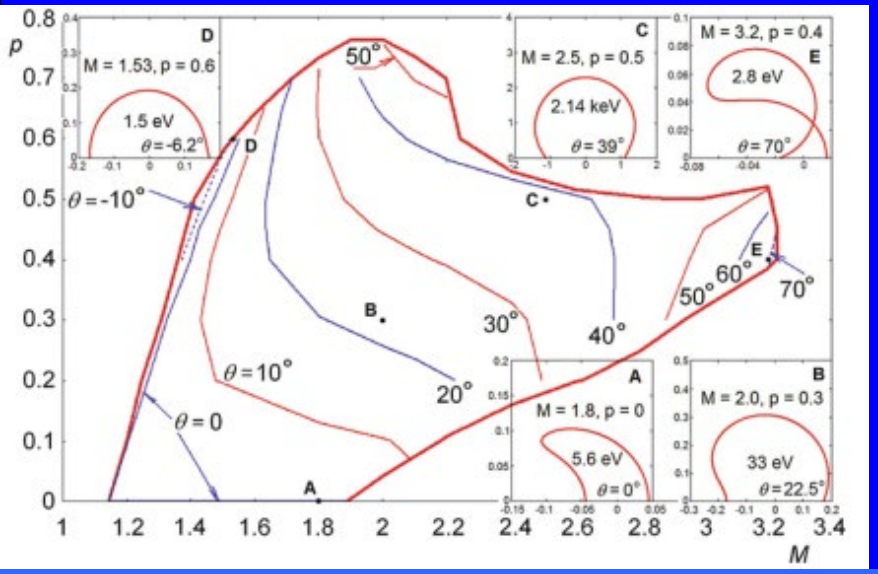

$M = eB_0/m\omega$ is the field parameter,
$p = \beta/(\alpha + \beta)$ can be named a geometrical parameter of the cavity.
Each cavity shape has its own p. Moving along the line p = const, (see the graph on the left-up) we have different energy of primary electrons. MP starts when this energy E_p is high enough for SEY > 1.
The incidence angle of the impacting electrons is important: the SEY grows when the electrons hit the surface at an angle < 90 deg.
If the electron has an initial phase and position different from the equilibrium ones, after the flight to the next impinge onto the surface, its phase and position should deviate less from the equilibrium. This is a condition of stability (simplified).

Multipactor on the cavity equator. Empirical formulae for multipacting fields

The formula for the magnetic parameter $M = eB_0/m\omega$ can be rewritten in the form $B_0 = 35.7 \cdot M \cdot f$ [GHz] (*)

The first formula of this kind was offered by W. Weingarten, the discoverer of the equatorial multipactor. Later, several authors offered analogous formulae with different coefficient before ***f***.

Table 8.2 Empirical formulae for the multipacting fields and corresponding values of M

Author	Formula	M calculated from (8.20)
Weingarten (1984) [7]	B [mT] = 72 f [GHz]	2.02
Fabbricatore et al. (1995) [24]	B [mT] = 78 f [GHz]	2.18
	B [mT] = 55 f [GHz]	1.54
	B [mT] = 57 f [GHz]	1.60
Saito (2001) [22]	B [mT] = 60 f [GHz]	1.68
Geng (2003) [25]	B [mT] = 5 + 55 f [GHz]	1.54 +0.14/f

Formula (*) generalizes the phenomenological formulae because it reflects dependence on geometry, i.e., the field parameter M is defined by the geometrical parameter p. For example, for most probable MP, see the previous slide, $M = 2.0$ for $p = 0.27$ or $M = 2.1$ for $p = 0.33$. Now, the coefficient before ***f*** obtains a physical meaning. This formula can be rewritten in a more practical way:

$$E_0 = \frac{B_0(1+\varepsilon)}{B_{pk}/E_{acc}} = \frac{35.7 \cdot M \cdot f}{B_{pk}/E_{acc}} \text{ [units are MV/m, GHz, mT].}$$

E_0 is the accelerating field corresponding to the presence of MP, B_0 is the magnetic field at the equator.

Multipactor on the cavity equator. Condition of stability

In the case when multipacting occurs near the cavity equator, the starting electron should be described both by the phase of the field and the distance from the equator because the electric field E_y changes with distance x. If the electron has an initial phase and position different from the equilibrium ones, after the flight to the next impinge onto the surface, its phase and position will change:

$$\Delta\theta_2 = (\partial\theta_2/\partial\theta_1)\Delta\theta_1 + (\partial\theta_2/\partial x_1)\Delta x_1,$$

$$\Delta x_2 = (\partial x_2/\partial\theta_1)\Delta\theta_1 + (\partial x_2/\partial x_1)\Delta x_1,$$

$$\begin{pmatrix}\Delta\theta_2\\ \Delta x_2\end{pmatrix} = \begin{pmatrix}a & b\\ c & d\end{pmatrix}\begin{pmatrix}\Delta\theta_1\\ \Delta x_1\end{pmatrix} \equiv A\begin{pmatrix}\Delta\theta_1\\ \Delta x_1\end{pmatrix}$$

$$\begin{pmatrix}\Delta\theta_{N+1}\\ \Delta x_{N+1}\end{pmatrix} = A^N\begin{pmatrix}\Delta\theta_1\\ \Delta x_1\end{pmatrix}$$

$$\lim_{N\to\infty} A^N = 0$$

$$\det|A-\lambda I| = 0.$$

$$|\lambda_1| < 1, \quad |\lambda_2| < 1.$$

```
N ← 1000
ε ← 10^-12
Δx ← -1·10^-6
Δθ ← -1·10^-4
[x0; θ0] ← [-6.195001·10^-1; 3.635428·10^-1]
θ0 ← θ0·π
θf ← θ0+1.1·π
xf0 ← -x0
m ← 0
while (|x0+xf0| > ε ∨ m = 0)
    x0 ← -xf0
    Y ← [x0; 0; 0; 1.027·10^-1]
    D(θ,Y) ← [Y_2; M·((1-p)·Y_3·sin(θ) - Y_4·cos(θ)); Y_4; M·(-p·Y_1·sin(θ) + Y_2·cos(θ))]
    S ← rkfixed(Y, θ0, θf, N, D)
    n ← 2
    while S_{n+1,4}·S_{n,4} > 0
        n ← n+1
    θf0 ← S_{n,4}·(S_{n+1,1} - S_{n,1}) ÷ (S_{n,4} - S_{n+1,4}) + S_{n,1}
    xf0 ← S_{n,4}·(S_{n+1,2} - S_{n,2}) ÷ (S_{n,4} - S_{n+1,4}) + S_{n,2}
    x2f ← S_{n,4}·(S_{n+1,3} - S_{n,3}) ÷ (S_{n,4} - S_{n+1,4}) + S_{n,3}
    y2f ← S_{n,4}·(S_{n+1,5} - S_{n,5}) ÷ (S_{n,4} - S_{n+1,4}) + S_{n,5}
    θ0 ← θf0 - π
```

```
= [6.195001·10^-1
   3.635428·10^-1
   9.185176·10^-1
   -6.516038·10^-1
   9.100000·10
   9.185176·10^-1
   6.516038·10^-1
   -4.415683·10^-1
   -5.589016·10^-1]
```

A fragment of a MathCAD program for calculation of $\lambda 1$ and $\lambda 2$.

An example of Runge-Kutta calculation of a trajectory.

$$Y := \begin{bmatrix}-6.195001\\ 0\\ 0\\ 1.027\cdot10^{-1}\end{bmatrix} \qquad \theta 0 = 1.142103$$

$$D(\theta, Y) := \begin{bmatrix}Y_2\\ M\cdot\left((1-p)\cdot Y_3\cdot\sin(\theta) - Y_4\cdot\cos(\theta)\right)\\ Y_4\\ M\cdot\left(-p\cdot Y_1\cdot\sin(\theta) + Y_2\cdot\cos(\theta)\right)\end{bmatrix}$$

$S := \text{rkfixed}(Y, \theta 0, \theta f, N, D)$

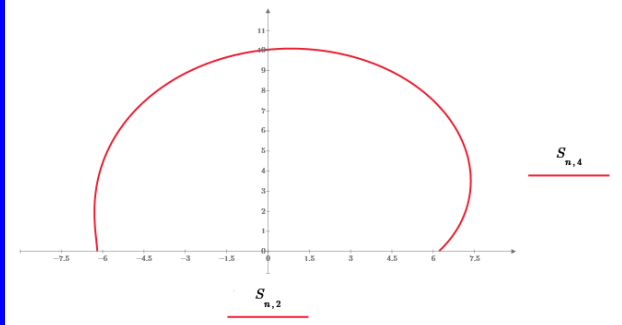

Multipactor on the cavity equator (2)

A handy way of fast calculation of the parameter *p* is shown in this Figure.

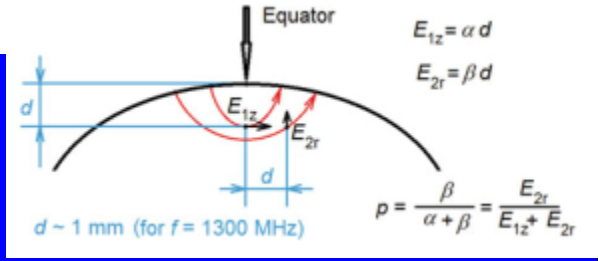

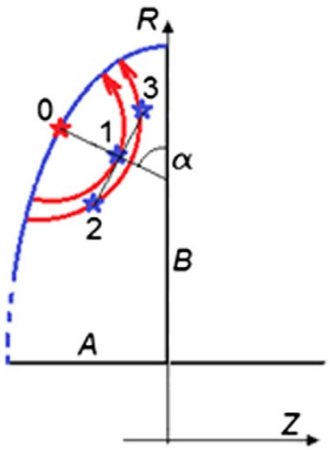

If the cavity cell is asymmetric, e.g. the end cell of a multicell cavity, the minimum of the electric field can shift from the equator, for example, to the point 0, then we need to erect a perpendicular to this point of the ellipse and find the fields at the distance *d*, at point 1, and in the points on a straight line parallel to the tangent at the point 0 at a distance *d* from the point 1, at points 2 and 3.

The software for the calculation of cavities gives usually **Er** and **Ez** components of the electric field. We need to have field components parallel or normal to the tangent at point 0. Let us call them analogously to the fields in the definition of *p* as E'_{2r} and E'_{1z}
This transformation looks as follows:

$$E'_r = E_r \cos\alpha - E_z \sin\alpha,$$

$$E'_z = E_r \sin\alpha + E_z \cos\alpha.$$

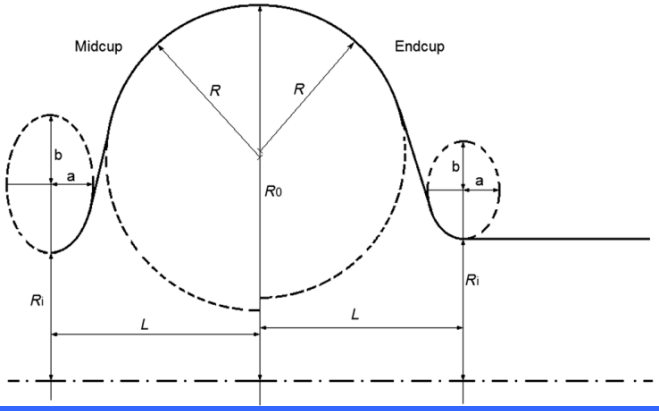

Example. End cell of the TESLA cavity.
Calculations for the end cell 2 give a shift ΔZ = −0.195 mm and α = 0.266° for the min *E*s. On the normal to the equator, we can find p_2 = 0.240 and p_3 = 0.327, but after the correction to the offset point p_2 = 0.285 and p_3 = 0.286. This calculation was repeated with a twice denser mesh (224×172 instead of 112×86). Now the shift was ΔZ = −0.205 and $p_2 = p_3$ = 0.286 with an accuracy of three decimal places.

1-point multipactor in crossed field of rf cavities

This was for the equator region (2-point MP)

$$B_z = -B_0 \cos\theta,$$
$$E_x = \alpha \cdot y \cdot \sin\theta,$$
$$E_y = -\beta \cdot x \cdot \sin\theta.$$

$$x'' = M[(1-p)y\sin\theta - y'\cos\theta],$$
$$y'' = M(-px\sin\theta + x'\cos\theta).$$

Equations of motion are the same

$$e\,(E_x + \dot{y}B_z) = m\ddot{x},$$
$$e\,(E_y - \dot{x}B_z) = m\ddot{y}.$$

$$\dot{x} = \omega x', \quad \ddot{x} = \omega^2 x'', \text{ and so on,}$$

This is for the flat wall (1-point MP)

$$E_x = -\alpha y \sin\theta,$$
$$E_y = E_s(x)\sin\theta$$
$$B_z = B_0\cos\theta.$$

$$x'' = M[(dq/dx - 1)y\sin\theta + y'\cos\theta],$$
$$y'' = M[q(x)\sin\theta - x'\cos\theta].$$

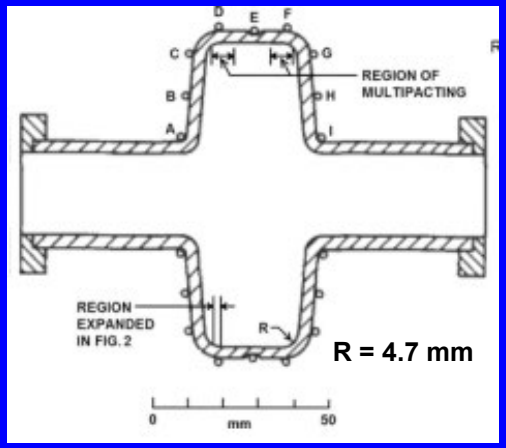

$$q = E_0/\omega B_0$$

q is a new geometrical parameter

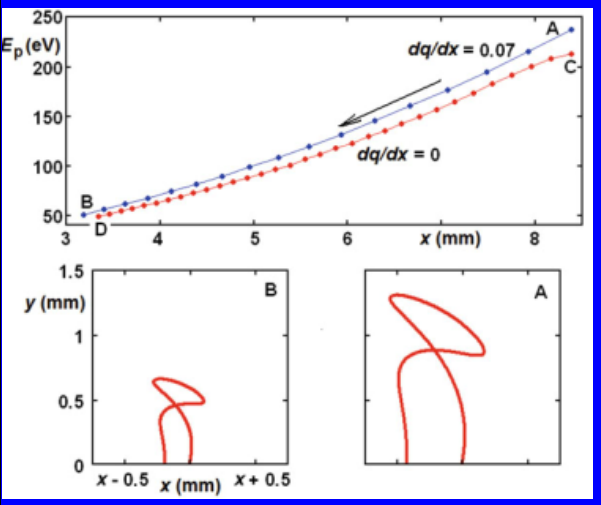

If q > 0, the 1-point MP is resonant as far as the phase stability is concerned, but the point of impact continuously shifts toward the equator. We can name this phenomenon "traveling multipactor".

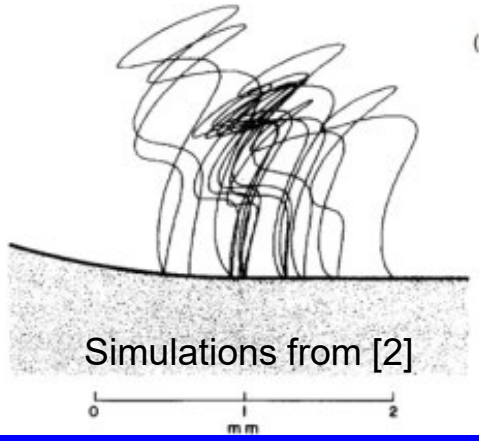

Simulations from [2]

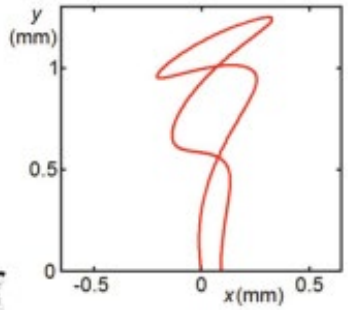

My solution of Eqs. of motion

[1] C.M. Lyneis et al., Appl. Phys. Lett. **1** (8), 541 (1977) – geometry. [2] I. Ben-Zvi et al., Proc. of PAC1973, p. 54 – simulations.

1-point multipactor in crossed field of rf cavities (2)

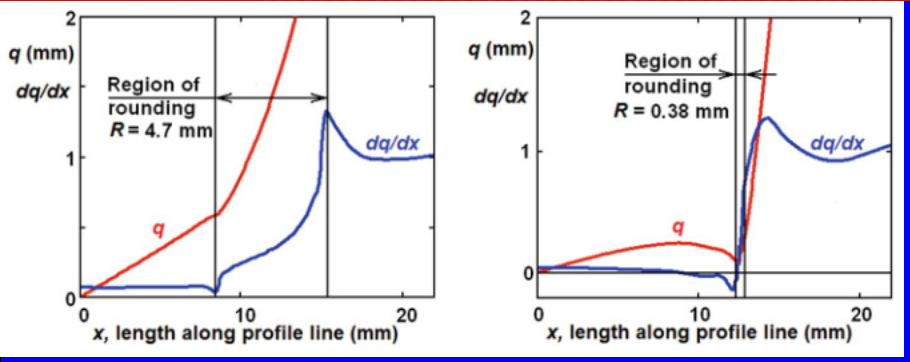

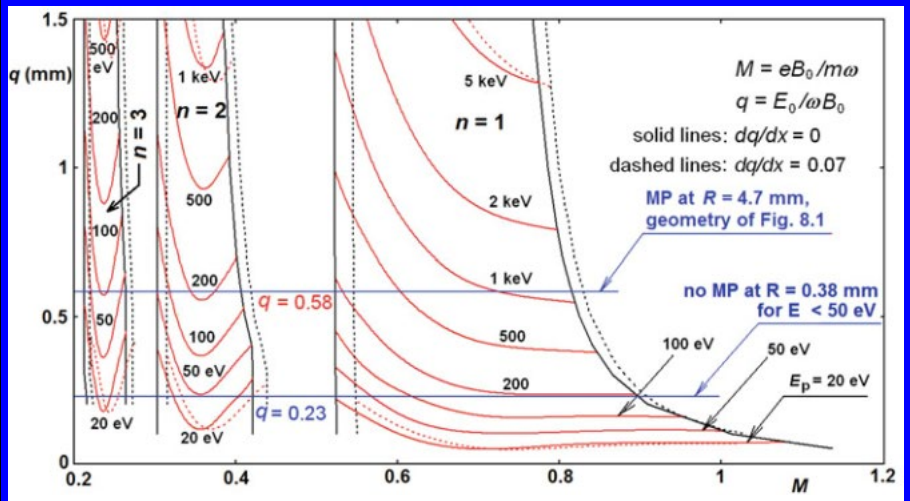

First 3 zones of MP1 with dq/dx = 0, and dq/dx = 0.07. Emission energy of secondary electrons Es = 4 eV; Ep is the impact energy of primary electrons.

One of the conclusions in the paper [2] was the following: the "electron avalanche multiplication effect…is not resonant in nature" . One can see a contradiction in this statement with the results from [1], where it is shown that "the multipacting is limited to discrete field levels". The question arises: if these levels are not resonances, why they are discrete?

The traveling feature of MP1 was not noticed in [2] as it was masked by many details taken into account, such as distributed start velocities, reflected electrons, and simply because too many trajectories are simultaneously shown in figures. Although these details show the real situation, they act like noise, hiding the main features of the phenomenon.
Therefore, MP1 is resonant in nature, but this is only a phase resonance as the MP travels along the cavity profile line toward the equator.

For the S-band cavity under consideration, $p = dq/dx = 0.07$, and hence MP2 does not happen at its equator as p is too low, << 0.3. On the other hand, the elliptical cavities have big p, TESLA has $p = 0.28$, Cornell ERL has $p = 0.28$, and MP1 is unlikely in such cavities.

[1] C.M. Lyneis et al., Appl. Phys. Lett. **1** (8), 541 (1977) – geometry. [2] I. Ben-Zvi et al., Proc. of PAC1973, p. 54 – simulations.

Multipacting-free cavities and transitions between cavities and beam pipes

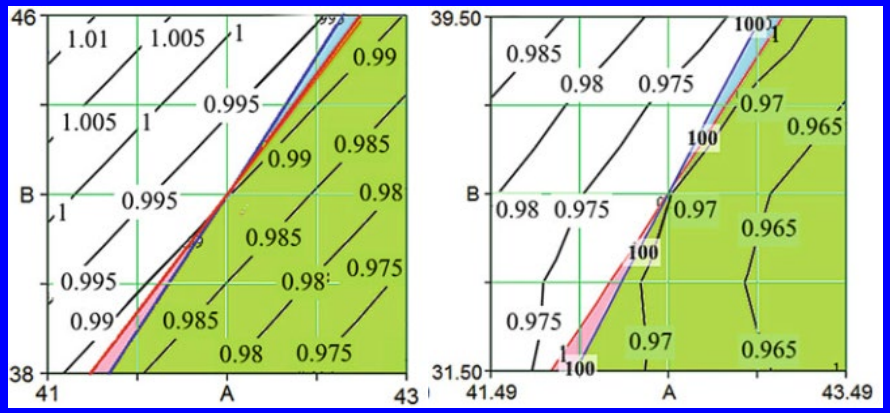

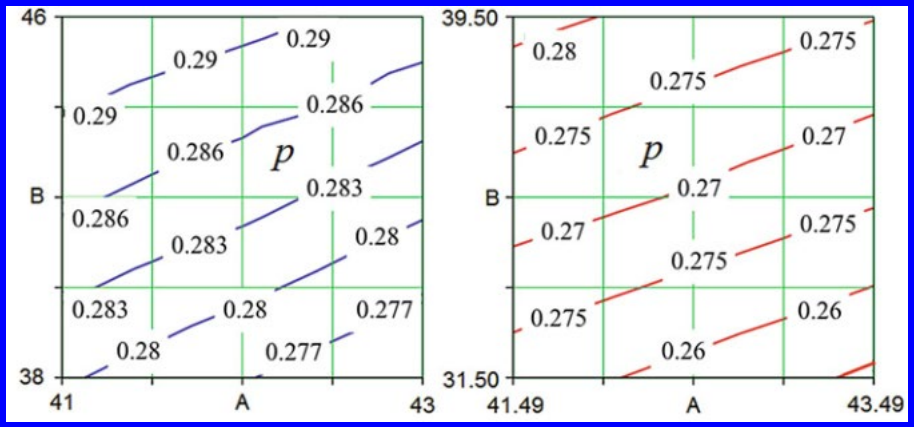

Returning to slides about optimization of the TESLA cavity, let us plot values of *p* for the same geometry. We can see that moving along the boundary of “forbidden areas”, we can decrease *p* below critical values, increasing *h* not more than by 0.5 %.

Multipacting-free cavities and transitions between cavities and beam pipes (2)

Tests of the Cornell ERL injector cavity (R.L. Geng, PAC2007) and KEK Ichiro cavity (Y. Morozumi,KEK notes, 2007) showed relatively strong MP, which was later attributed through computer simulations and experimentally to the transition region between the cavity end cells and beam pipes.

We proposed an explanation that an electric field minimum is associated with the local potential well, thus attracting electrons to its location and creating conditions favorable to multipacting.

Multipacting simulation for a cavity with an inner corner rounded with R = 9 mm

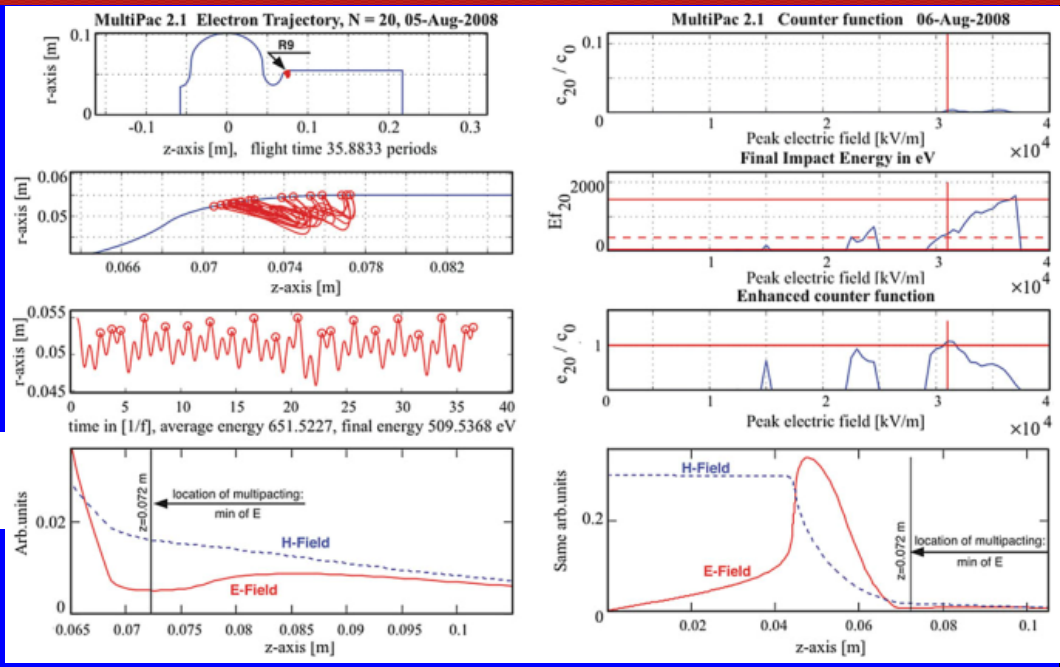

Minimum becomes shallow at R = 18 mm and disappears at R = 36 mm. No multipactor in both cases.

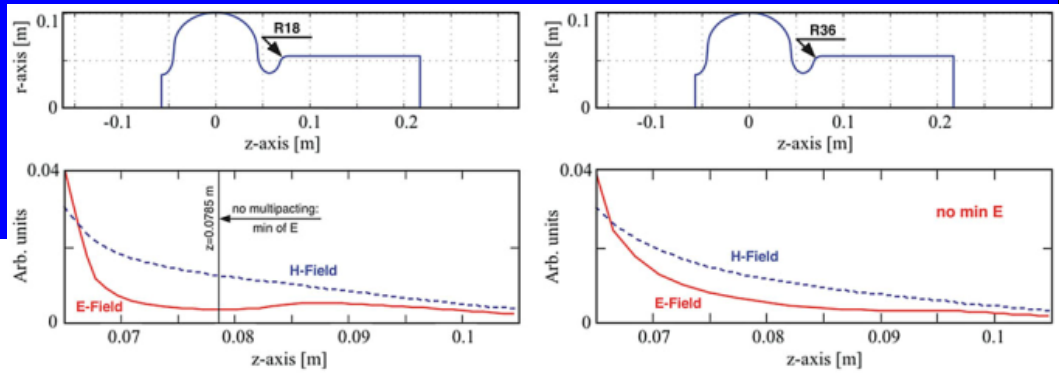

Mechanism of the motion to the min E

Motion of electrons near the minimum RF electric field can be explained by the mechanism suggested in [*]. According to this work, acceleration of electrons in an RF field is defined by

$$\ddot{\mathbf{r}}_0 = -\nabla\Phi, \quad \Phi = (\eta/2\omega)^2|\mathbf{E}|^2,$$

where $\eta = e/m$, $r_0(t)$ is a slowly varying function (in terms of the RF oscillation period), as distinguished from an oscillating function $r_1(t) = A \sin \omega t$ (we omit terms connected with initial position and velocity), and Φ is the potential proportional to the square of the electric field amplitude. Function $r_1(t)$ is assumed to be much smaller than the distance over which the amplitude of the RF field changes significantly. As one can see from the above expression, electrons are pushed to the region of lower electric field amplitude (so-called Miller force).

One can imagine the behavior of electrons in the cavity electric field region as an electron wind blowing in the direction from the iris to the beam pipe. In a “calm corner” behind the iris, electrons can accumulate and multipactor can emerge if the SEY is high enough.

The potential well theory can be successfully applied to coaxial or waveguide transmission lines. This force explains drift of multipacting electrons from the waveguide midline to the sidewalls, or migration to the standing wave minimum.

[*] A. V. Gaponov, M. A. Miller, Potential well for charged particles in a high-frequency electromagnetic field. Sov. Phys. JETP **7**, 168 (1958).

Conclusion

- We discussed a method of search of geometrical parameters of elliptical cavities to obtain the best possible figures of merit: Bpk/Eacc and GR/Q for given Epk/Eacc, aperture, wall slope angle. The result of this search is the reentrant cavity with a record acceleration rate of 59 MeV/m with the aperture radius of 30 mm and 52 MeV/m with 35 mm.
- Further improvement in optimization is offered – equidistant optimization, that makes clear the dependence of maximal acceleration gradient on the limiting electric and magnetic field.
- Use of specially developed software – TunedCell on the base of SuperLANS - made possible to find best geometries of cavities in a 4D space of parameters.
- An overview of different multipactor kinds is presented, zones of 1-point and 2-point multipactor in elliptical cavities are described, and a method of search for multipactor–free geometries is offered.

Acknowledgements

I am thankful to

- Hasan Padamsee for his idea about sacrificing *E*pk to decrease *H*pk, and his support at the first stage of this work
- Dmitry Myakishev for his special version of SLANS for optimization, and the envelope programs: TunedCell etc.
- Gianluigi Ciovati for this invitation
- And I am thankful to you all for your attention